Independent endothelial functions of PIEZO1 and TRPV4 in hepatic portal vein and predominance of PIEZO1 in mechanical and osmotic stress

Naima Endesh[1], Eulashini Chuntharpursat-Bon[1], Charlotte Revill[2], Nadira Y. Yuldasheva[1], T. Simon Futers[1], Gregory Parsonage[1], Neil Humphreys[3], Antony Adamson[3], Lara C. Morley[1], Richard M. Cubbon[1], K. Raj Prasad[4], Richard Foster[2], Laeticia Lichtenstein[1]*, David J. Beech[1]

[1]School of Medicine and [2]School of Chemistry, University of Leeds, Leeds, LS2 9JT, UK. [3]Faculty of Biology, Medicine and Health, University of Manchester, AV Hill Building, Manchester M13 9PT, UK. [4]Department of Hepatobiliary and Transplant Surgery, St James's University Hospital, Leeds, UK.

*Corresponding author: Dr Laeticia Lichtenstein, Leeds Institute of Cardiovascular and Metabolic Medicine, LIGHT Building, Clarendon Way, School of Medicine, University of Leeds, Leeds LS2 9JT, UK. E-mail l.lichtenstein@leeds.ac.uk.

Electronic word count

4268 words

Figures and tables

This manuscript contain 7 figures, and 7 supplementary figures.

Abbreviations

Transient Receptor Potential Vanilloid (TRPV), nitric oxide synthase (NOS), tamoxifen (TAM), acetylcholine (ACh), phenylephrine (PE), N^{ω}-Nitro-L-arginine methyl ester hydrochloride (L-NAME), dimethyl sulphoxide (DMSO), prostaglandin (PG), apamin (Apa), charybdotoxin (ChTx), 50% inhibition (IC_{50}s), phospholipase A (PLA), cyclooxygenase (COX), endothelium-derived hyperpolarisation (EDH).

Conflict of interest disclosure

The authors declare no conflicts of interest other than obligations from their research grants (Financial Support).

Funding statement

The work was supported by research grants from Wellcome (grant number 110044/Z/15/Z) and British Heart Foundation (grant number RG/17/11/33042). For the purpose of Open Access, the authors have applied a CC BY public copyright license to any Author Accepted Manuscript version arising from this submission.

Experimental animal studies

All work with mice occurred under the authority of the University of Leeds Animal Welfare and Ethical Review Committee and UK Home Office Project Licences P606320FB and PP8169223. All animals received human care and the study protocols comply with our institution's guidelines. Animal experiments conformed to the Animal Research: Reporting of *In Vivo* Experiments (ARRIVE) guidelines (http://www.nc3rs.org.uk/arrive-guidelines), developed by the National Centre for the Replacement, Refinement and Reduction of Animals in Research (NC3Rs) to improve standards and reporting of animal research.

Abstract

Background & aims: PIEZO1 and TRPV4 are mechanically and osmotically regulated calcium-permeable channels. The aim of this study was to determine the relevance and relationship of these channels in contractile tone of hepatic portal vein, which experiences mechanical and osmotic variations as it delivers blood to the liver from the intestines, gallbladder, pancreas and spleen.

Methods: Wall tension was measured in freshly dissected portal vein from adult male mice, which were genetically unmodified or modified for either a non-disruptive tag in native PIEZO1 or endothelial-specific PIEZO1 deletion. Pharmacological agents were used to activate or inhibit PIEZO1, TRPV4 and associated pathways, including Yoda1 and Yoda2 for PIEZO1 and GSK1016790A for TRPV4 agonism respectively.

Results: PIEZO1 activation leads to nitric oxide synthase- and endothelium-dependent relaxation of the portal vein. TRPV4 activation causes contraction, which is also endothelium-dependent but independent of nitric oxide synthase. The TRPV4 mediated contraction is suppressed by inhibitors of phospholipase A_2 and cyclooxygenases, and mimicked by prostaglandin E_2, suggesting mediation by arachidonic acid metabolism. TRPV4 antagonism inhibits the effect of agonising TRPV4 but not PIEZO1. Increased wall stretch and hypo-osmolality inhibit TRPV4 responses while lacking effects on or amplifying PIEZO1 responses.

Conclusions: Portal vein contains independently functioning PIEZO1 channels and TRPV4 channels in endothelium, the pharmacological activation of which leads to opposing effects of vessel relaxation (PIEZO1) and contraction (TRPV4). In mechanical and osmotic strain, the PIEZO1 mechanism dominates. Modulators of these channels could present important new opportunities for manipulating liver perfusion and regeneration in disease and surgical procedures.

Key words

Hepatobiliary system, Liver, Portal vein, Vein, Vasculature contraction, Vascular relaxation, Endothelium, Calcium signalling, Calcium-permeable channel, Non-selective cation channel, PIEZO channel, Transient Receptor Potential Vanilloid 4 (TRPV4) channel, Nitric oxide, Arachidonic acid metabolism, Mechanical force, Osmolality, endothelial nitric oxide synthase.

Graphical abstract

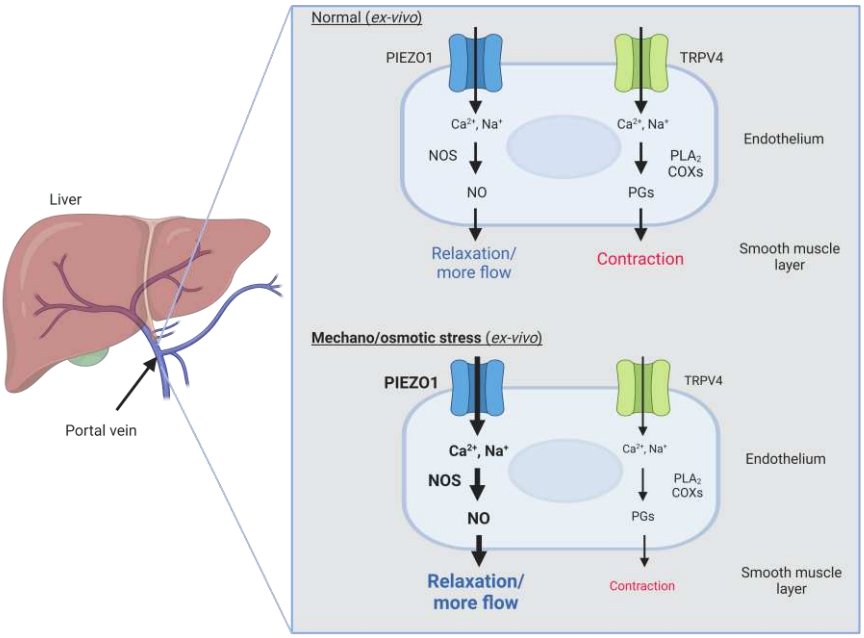

Lay summary/ Keypoints

Proteins that control the liver's blood flow are important in liver physiology, liver disease, the treatment of liver disease and the recovery of the liver after medical and surgical interventions. Here we identify proteins that control the diameter of the portal vein, which controls the majority of blood flow to the liver. We show how the proteins serve different functions and that one becomes more important as mechanical and osmotic strains occur on the vessel. We show the effectiveness of activating the proteins by specific chemicals and suggest the potential for new therapeutic drugs based on these molecules to achieve new ways for beneficial liver modulation.

1. PIEZO1 channel agonism causes nitric oxide synthase- and endothelium-dependent relaxation of portal vein

2. TRPV4 channel agonism causes phospholipase A_2-, cyclooxygenases 1 and 2- and endothelium-dependent contraction of portal vein that is mimicked by prostaglandin E_2

3. TRPV4 antagonism inhibits the effect of TRPV4 agonism but not PIEZO1 agonism, suggesting separation of TRPV4 from PIEZO1

4. Increased wall stretch and hypo-osmolality inhibit TRPV4 while lacking effects on or amplifying PIEZO1

5. New mechanistic insight and ways to pharmacologically modulate the liver's blood flow are suggested

Introduction

The hepatic portal vein links capillary beds, carrying blood from the microvasculatures of the gastrointestinal tract, spleen, pancreas and gallbladder to the microvasculature of the liver [1]. It accounts for about 75% of liver blood flow, branching and feeding into the sinusoids for first-pass metabolism and detoxification of blood contents by hepatic mechanisms and the delivery of key regulators such as glucagon to control gluconeogenesis [2]. It is an active vessel, helping to propel or restrict blood flow to the liver and modulating changes in the liver such as its regeneration by altering shear stress and stimulating angiogenesis [3]. The vein is lined by endothelium, has a medial layer containing smooth muscle cells arranged circularly and longitudinally, and is innervated [4-6]. Its contractile properties are influenced by chemical factors including noradrenaline, acetylcholine and angiotensin II [6] and mechanical and osmotic factors arising from changes in vessel length, wall tension, blood flow and blood water content [7-10]. Flow through the portal vein increases or decreases physiologically, for example after a meal or during physical exercise [10]. Osmolality decreases in portal blood after the drinking of water [11]. Portal vein physiology changes in pathology and in the treatment of disease [12]. There are rare diseases of the portal vein that include congenital portal venous shunts, aneurysms and portal vein thrombosis. Common diseases of liver that result in cirrhosis and portal hypertension include alcoholic and non-alcoholic steatohepatitis [1,13]. Portal pressure may also increase after liver resection and other surgery when normal blood flow occurs into a smaller liver [14], potentially triggering regeneration via nitric oxide signalling [3].

The sensing of mechanical forces in biology is multifactorial and still poorly understood [15]. While entire cellular systems involving many proteins, lipids and other factors are likely to be important [15], the discovery of PIEZO proteins, recognised by the 2021 Nobel Prize for Medicine or Physiology, has suggested that proteins exist that are specialised for force detection at the core of this biology [16-18]. The PIEZO proteins form trimeric ion channels of almost a million Daltons, each with 114 (3x38) membrane-spanning segments [19,20]. They locate particularly to the plasma membrane and integrate with membrane lipids where they respond in milliseconds to mechanical stimuli, enabling transmembrane ionic currents and raising the concentration of cytoplasmic calcium ion (Ca^{2+}), the pivotal second messenger. Although it may not be a primary stimulator, decreased osmolality may

activate the channels or enhance their response to mechanical force [21,22]. The PIEZO1 protein is expressed in the endothelium where it is a critical sensor of shear stress [23-27]. It integrates physiological force with vascular architecture[24], regulates blood pressure [25,27], maintains muscle capillary density [28], enables physical exercise performance [28], drives angiogenesis [24,29], regulates endothelial permeability [30,31] and determines the phosphorylation and stability of endothelial nitric oxide synthase (NOS3/eNOS) [24,27,28], amongst other effects [23]. PIEZO1 is in other cell types too, including vascular smooth muscle cells [32] and nerve endings that control blood pressure [33]. Relevance to hepatic vasculature is emerging. PIEZO1 is functional in microvascular endothelial cells of mouse and human liver [24,25,34] where it stimulates ADAM10 protein and NOTCH1 signalling [34]. It is a suggested mediator of portal hypertension through expression of neutrophil chemoattractant CXCL1 [35]. A novel PIEZO1 agonist, Yoda2, relaxes portal vein via endothelial PIEZO1 and NOS3 activity [36].

Another channel linked to vascular mechanical and osmotic responses is the TRPV4 channel [37]. Like PIEZO1, TRPV4 is a Ca^{2+} permeable non-selective cation channel [37]. TRPV4 channels participate in endothelial responses to shear stress [38,39] and have many vascular roles [40] but, contrasting with PIEZO1, they are not clear mechanical sensors but instead apparently integrate the sensing of multiple chemical factors that include arachidonic acid metabolites [41]. In cultured human umbilical vein endothelial cells, TRPV4 is downstream of PIEZO1, activating after stimulation of phospholipase A_2 to amplify the intracellular Ca^{2+} signal originally triggered by PIEZO1 [42].

Here we sought to determine the relevance and relationship of PIEZO1 and TRPV4 in contractile tone of hepatic portal vein. We find both to be functionally important and acting via endothelium-dependent mechanisms, yet they are opposing and apparently independent in their effects. Although we expected TRPV4 to be downstream of PIEZO1, amplifying its regulation of contractile tone, we find no evidence for this. Moreover, we suggest that PIEZO1 and TRPV4 are regulated differently by mechanical and osmotic stress, with PIEZO1 predominating when there is increased mechanical and osmotic stress.

Materials and Methods

Animals 10-14 week-old C57BL/6J male mice were used for experiments. Only male mice were used in order to reduce variability that might arise due to sex differences and reproductive cycle. Mice were housed in GM500 individually ventilated cages (Animal Care Systems), at 21°C, 50–70% humidity, with a 12/12 hr light/dark cycle. They had ad libitum access to RM1 diet (Special Diet Services, Witham, UK) with bedding from Pure'o Cell (Datesand, Manchester, UK). All work with mice occurred under the authority of the University of Leeds Animal Welfare and Ethical Review Committee and UK Home Office Project Licences P606320FB and PP8169223. The number of cage companions was up to 5. Animals were visually inspected and weighed at a minimum of weekly intervals for welfare-related assessments. Local animal welfare advice and steps were taken in the rare cases of concern for an animal or animals. The genetically modified mice did not display any obvious adverse effects. Animals weighed 25-35 g. Genotypes were determined by a service using real-time PCR with specific probes designed for each gene (Transnetyx, Cordova, TN). C57BL/6 J mice with PIEZO1 gene flanked with LoxP sites ($PIEZO1^{flox}$) and tamoxifen (TAM)-induced disruption of the PIEZO1 gene in the endothelium were described previously [43]: In brief, $PIEZO1^{flox/flox}$ mice were crossed with mice expressing cre recombinase under the Cadherin5 promoter (Tg(Cdh5-cre/ERT2)1Rha and inbred to obtain $PIEZO1^{flox/flox}$/Cdh5- cre mice [43]. TAM (Sigma-Aldrich) was dissolved in corn oil (Sigma-Aldrich) at 20 mg mL^{-1}. Mice were injected intra-peritoneally with 75 mg kg^{-1} TAM for 5 consecutive days and studies were performed 10–14 days later. $PIEZO1^{flox/flox}$/Cdh5-cre mice that received TAM injections are referred to as $PIEZO1^{\Delta EC}$. $PIEZO1^{flox/flox}$ littermates (lacking Cdh5-cre) that received TAM injections were the controls (control genotype). Mice were aged to 10 weeks before the deletion occurred. TAM injections and genotyping were performed by a researcher (T.S.F.) independently from the myographer (N.E.) such that the genotypes were blind to the myographer. The different genotypes were studied at random as they became available, depending on the genotypic spread of each litter. Before experiments, mice were culled by cervical dislocation according to Schedule 1 procedure approved by the UK Home Office.

HA-PIEZO1 mice Mice with hemagglutinin (HA) tag in native PIEZO1 (PIEZO1^{HA} mice) were generated by introducing HA sequence between amino acids A2439 and D2440 by CRISPR-Cas9. A sgRNA was selected based on proximity to the target region and low off-targeting potential (catcgagctgcaggactgca-agg) and an ssDNA repair template with the HA tag sequence and 60nt flanking homology arms designed to facilitate integration of the HA tag sequence after Cas9 induced double strand break was synthesised (Integrated DNA technologies, with PAGE purification). sgRNA sequence was synthesised as an Alt-R crRNA (Integrated DNA Technologies) oligo and re-suspended in sterile Opti-MEM (Gibco) and annealed with tracrRNA (Integrated DNA Technologies) by combining crRNA (2.5 µg) with tracrRNA (5 µg) and heated to 95 °C. After annealing the complex, an equimolar amount was mixed with Cas9 recombinant protein (1500 ng) (NEB), the ssDNA repair template (final concentration 10 ng·µL^{-1}) in Opti-MEM (total volume, 15 µL) and incubated (RT, 15 min). Mouse embryos were electroporated (Nepa21 electroporator, Sonidel) using AltR crRNA:tracrRNA:Cas9 complex (200 ng·µL^{-1}; 200 ng·µL^{-1}; 200 ng·µL^{-1} respectively) and ssDNA HDR template (500 ng·µL^{-1}) [44]. Zygotes were cultured overnight, and the resulting 2-cell embryos surgically implanted into the oviduct of day 0.5 post-coitum pseudopregnant mice. After birth and weaning, genomic DNA extracted using REDExtract-N-Amp™ tissue PCR kit (Sigma) was used to genotype pups by PCR using primers cgactctaactatcccactcaac and atccctctgcagtactcacc, followed by Sanger sequencing of candidate pup1. Mice were bred to obtain homozygotes for HA-tag-PIEZO1 (PIEZO1^{HA} mice).

Myography Portal veins were isolated from mice and transferred to gassed (95% O_2 and 5% CO_2) Krebs solution, which comprised (in mM): NaCl 130, KCl 4.7, $CaCl_2$ 1.16, KH_2PO_4 1.18, $MgSO_4(7H_2O)$ 1.7, $NaHCO_3$ 14.9, EDTA 0.026 and glucose 5.5 (pH 7.4). Vessels were carefully cleaned of fat and connective tissue under a dissecting microscope and cut into 1 mm-long segments. These segments were mounted on two stainless steel wires in chambers of a myograph (Multi Wire Myograph System 620 M) filled with 5 mL Krebs solution maintained at 37 °C. The resting tension of each segment was determined by the normalization module of Danish Myo Technology Normalization Module LabChart 8 to achieve tensions specified Results. This was done by gradual distention of the segments by increasing separation of the jaws of the myograph in a stepwise manner. LabChart 8 calculated the tension-force relationship for the portal vein segments. Then, the segments were equilibrated for 60 min prior to experiments. Contractile viability was examined by applying 60 mM K^+ solution prepared by exchanging NaCl with an equimolar amount of KCl; this K^+ concentration depolarises the smooth muscle cells, opening voltage-gated Ca^{2+} channels and thereby causing contraction, the amplitude of which was taken as a reference in some cases. Endothelial integrity was examined by adding acetylcholine (ACh) at 0.3, 1, 3 and 10 µM once the phenylephrine (PE) contractile response had reached its plateau. Segments were only used for investigation if they constricted in response to PE and dilated in response to Ach (unless endothelium was deliberately removed). Endothelial denudation was achieved by luminal rubbing of the vein on a stainless-steel cannula and passing of air bubbles in Krebs solution through the lumen before mounting segments on wires for tension recording. Removal of endothelium was considered successful if the segment relaxed less than 10% when exposed to 10 µM ACh. The osmolality of Krebs solution (indicated above) was 282 mOsm.kg^{-1}. Hypotonicity was achieved by decreasing the concentration of NaCl by 14 mM, generating modified Krebs solution containing (in mM): NaCl 116, KCl 4.7, $CaCl_2$ 1.16, KH_2PO_4 1.18, $MgSO_4$ $(7H_2O)$ 1.7, $NaHCO_3$ 14.9, EDTA 0.026 and glucose 5.5 (pH 7.4). The osmolality of the modified Krebs solution was 255 mOsm.kg^{-1}. The tonicity of solutions was measured using a freezing-point depression osmometer (Model 332, Advanced Instruments).

Immunostaining Wildtype (PIEZO1^{WT}) or PIEZO1^{HA} mice were anaesthetised under isoflurane (5 % induction and 2 % maintenance). Mice were perfused via the portal vein by syringe with PBS (10 ml), followed by 4 % PFA (20 ml). The aorta and portal vein from these mice were dissected. Permeabilisation and blocking of tissue was carried out using staining buffer (PBS pH 6.8, 0.5 % Triton, 0.01 % Na deoxycholate, 1 % BSA, 0.02 % NaN_3, 0.1 mM $CaCl_2$, 0.1 mM $MgCl_2$, 0.1 mM $MnCl_2$) containing 2 % goat serum (Agilent, CA, USA), overnight at 4 °C on an orbital shaker. Primary antibodies against CD31 (BD Pharmingen™, 550274, 1:100) and HA (Cell Signalling mAB3724, 1:100) were diluted in a 1:1 solution of PBS:staining buffer and incubated overnight at 4 °C on an orbital shaker. Aorta and portal vein tissues were rinsed in PBS with 0.25 % Triton (6x, 15 min) at room temperature. Goat secondary antibodies (Invitrogen A21246 and A-11006, 1:200) were diluted

in a 1:1 solution of PBS:staining buffer and incubated overnight at 4 °C on an orbital shaker in the dark. Excess antibody was removed by washing with PBS containing 0.25 % Triton (6 x, 15 min) at room temperature (RT). Tissues were washed in PBS prior to incisions to allow whole-mounting between a slide and coverslip using ProLong™ Gold (Invitrogen). Imaging was carried out on LSM710 (Carl Zeiss Ltd.). Images were exported to Fiji for final processing and assembly. Linear adjust of brightness and contrast was applied to the entire image. The intensity value for each image was normalised to the background.

Reagents All chemicals except Yoda1 were purchased from Sigma Aldrich and stored at -20 °C. PE (phenylephrine), ACh (acetylcholine) and L-NAME (N^{ω}-Nitro-L-arginine methyl ester hydrochloride) were dissolved in distilled water to make 100 mM stocks. GSK1016790A (*N*- [(1*S*)-1- [[4- [(2*S*)-2- [[(2,4-Dichlorophenyl)sulfonyl]amino]-3-hydroxy-1-oxopropyl]-1-piperazinyl]carbonyl]-3-methylbutyl]benzo [*b*]thiophene-2-carboxamide), GSK2193874 (3-([1,4′-Bipiperidin]-1′-ylmethyl)-7-bromo-N-(1-phenylcyclopropyl)-2- [3-(trifluoromethyl)phenyl]-4-quinolinecarboxamide), SC-560 (5-(4-Chlorophenyl)-1-(4-methoxyphenyl)-3-(trifluoromethyl)-1H-pyrazole), indomethacin, celecoxib (Celecoxib, 4- [5-(4-Methylphenyl)-3-(trifluoromethyl)-1H-pyrazol-1-yl]benzenesulfonamide) and bromoenol lactone (E-6-(Bromoethylene)tetrahydro-3-(1-naphthyl)-2H-pyran-2-one) were dissolved in dimethyl sulphoxide (DMSO) to make stock solutions of 10 mM. Prostaglandin E_2 (PGE_2), apamin (Apa) and charybdotoxin (ChTx) were dissolved in distilled water to make stock solutions of 10 mM. SIN-1 (3-Morpholinosydnonimine, HCl) was prepared as a 20 mM stock in DMSO. Yoda1 (2- [5- [[(2,6-Dichlorophenyl)methyl]thio]-1,3,4-thiadiazol-2-yl]-pyrazine) (Tocris) stock solution was 10 mM in DMSO. Yoda2 is a 4-benzoic acid derivative of Yoda1 [36]. It was synthesised in-house and prepared as a 10 mM stock solution in DMSO.

Data analysis Myography traces show readings taken every 0.5 or 1 s, smoothed with the Savitzky-Golay filter set to 70 points. Contractions are expressed as a percentage of 60 mM K^+-induced contraction. Relaxation responses are expressed as the percentage reversal of the phenylephrine contraction. EC_{50} (the concentration producing 50% of the maximal response) estimates from appropriately saturating concentration-response curves were fitted with a standard Hill equation. The data are expressed as mean ± standard deviation (SD) for at least 5 independent experiments (n) on portal vein segments from separate mice (e.g., n=5 indicates data from 5 mice). Paired or unpaired t-tests were used to compare two groups and one-way ANOVA followed by Tukey's test for multiple groups. Probabilities (*P*) of $*P < 0.05$, $**P < 0.01$ and $***P < 0.001$ are indicated for statistical significance. NS indicates no significant difference. All data were analysed by OriginPro 2020 (OriginLab).

Results

PIEZO1 causes relaxation via endothelial nitric oxide synthase In agreement with prior findings [36], the PIEZO1 agonist Yoda1 causes concentration-dependent relaxation of portal vein pre-contracted by α_1-adrenergic receptor agonist phenylephrine (PE) (Figure 1a). The effect is suppressed by conditional genetic deletion of PIEZO1 in endothelium ($PIEZO1^{\Delta EC}$) (Figure 1b, c), consistent with PIEZO1 being expressed in endothelium of portal vein based on immunostaining of a haemagglutinin (HA) tag incorporated in native PIEZO1 [45] (SI Figure S1). The generation of nitric oxide is likely to be a key event downstream of this PIEZO1 because nitric oxide synthase (NOS) inhibition by L-NAME suppresses the effect of Yoda1 (Figure 1d, e). After endothelial deletion of PIEZO1, L-NAME has no significant effect (SI Figure S2). The data suggest that activation of PIEZO1 in endothelium causes endothelium- and nitric oxide-dependent relaxation of portal vein.

TRPV4 causes contraction Selective TRPV4 pharmacology exists [46,47]. Application of GSK1016790A, a TRPV4 agonist [47], in the absence of PE-induced tone causes strong reversible contraction (Figure 2a, b) similar in magnitude and character to the contraction caused by PE (*cf* Figure 1a). The contraction is similar when GSK1016790A is washed out and then applied for a second time (Figure 2a). The effect is concentration dependent, with 50% maximum effect (EC_{50}) occurring at 0.7 nM (Figure 2b), which is in the potency range expected for TRPV4 [47]. The GSK1016790A effect is abolished by the TRPV4 antagonist GSK2193874[46] (Figure 2c).

GSK1016790A potentiates tone in the presence of PE and this effect is blocked by GSK2193874 (Figure 2d). The data suggest that TRPV4 activation causes contraction of portal vein.

TRPV4 effect depends on endothelium To determine if the TRPV4 agonist (GSK1016790A) effect is endothelium-dependent, the endothelium was physically removed. This was validated by measuring responses to acetylcholine, an endothelium-dependent vascular relaxant [48]. It was difficult to remove the endothelium without damaging the underlying smooth muscle but we observed a range of acetylcholine responses and examples in which the acetylcholine response was missing yet the PE response remained (Figure 3a, b), suggesting loss of endothelial but not smooth muscle function. We plotted the amplitude of the GSK1016790A effect against the amplitude of acetylcholine effect (Figure 3c). When there is no relaxation to acetylcholine or acetylcholine's effect is reversed into contraction, there is no effect of GSK1016790A (Figure 3c). When there is relaxation to acetylcholine, the amplitude of its relaxant response correlates positively with the amplitude of the contractile response to GSK1016790A (Figure 3c, right-hand panel). The data suggest that the TRPV4 effect is endothelium dependent.

TRPV4 effect does not involve common Ca^{2+}-dependent relaxant mechanisms TRPV4 forms Ca^{2+}-permeable channels that elevate intracellular Ca^{2+} [37]. We therefore tested for contributions of common Ca^{2+}-dependent endothelial relaxant mechanisms, which are nitric oxide synthase 3 (NOS3) and the small and intermediate conductance Ca^{2+}-activated potassium (K) channels (SK and IK). Such mechanisms may counter-balance the contractile effect of GSK1016790A. However, the NOS3 inhibitor L-NAME and the SK and IK inhibitors apamin and charybdotoxin have no effect on the GSK1016790A response (Figure 3d-f) despite abolishing the acetylcholine response (SI Figure S3). The data suggest that TRPV4 activation in endothelium does not evoke the NOS3 or SK/IK Ca^{2+}-dependent relaxant mechanisms.

TRPV4 effect is inhibited by cyclooxygenase (COX) inhibitors COX activity is a potential mediator of portal vein contraction [49]. COXs mediate endothelium-derived contraction by generating prostanoids that diffuse to the smooth muscle layer [50]. We tested if COX inhibitors affect the GSK1016790A response. SC-560 is selective for inhibition of COX1 over COX2, with concentrations for 50% inhibition (IC_{50}s) of 0.009 and 6.3 μM respectively [51]. SC-560 (1 μM) partly inhibits the GSK1016790A response (Figure 4a) and a 10-fold higher concentration (10 μM SC-560) has no further effect (SI Figure S4). SC-560 does not prevent PE-evoked contraction or acetylcholine-induced relaxation (SI Figure S4). Given that the non-selective COX inhibitor indomethacin abolishes the GSK1016790A response (SI Figure S4), we hypothesized that COX2 mediates the residual response. We therefore tested a COX2-selective inhibitor. Celecoxib (SC58635) inhibits COX1 and COX2 with IC_{50}s of 15.0 and 0.04 μM respectively [52]. The combination of SC-560 (1 μM) and celecoxib (10 μM) abolishes the GSK1016790A response (Figure 4b) without preventing PE or acetylcholine responses (SI Figure S4). The data suggest that COXs are required for the TRPV4 mediated contractile effect.

TRPV4 effect is inhibited by phospholipase A_2 inhibitor The substrate for COXs is arachidonic acid generated from membrane phospholipids by Ca^{2+}-dependent phospholipase A_2 activity [53]. An inhibitor of phospholipase A_2 is bromoenol lactone [54]. Bromoenol lactone (10 μM) abolishes the GSK1016790A response (Figure 4c) without affecting PE or acetylcholine responses (SI Figure S4). The data suggest that phospholipase A_2 activity mediates the TRPV4 contractile effect by generating arachidonic acid as a substrate for COX activity.

TRPV4 effect is mimicked by prostaglandin E_2 COXs generate prostanoids and several have contractile effects on smooth muscle[50]. Prostaglandin E_2 is found in portal vein [55]. We tested the effect of prostaglandin E_2 and observed concentration-dependent contraction (Figure 4d). The EC_{50} for the prostaglandin E_2 effect is 4 μM (Figure 4d). The data suggest that prostaglandin E_2 is a mimic and candidate mediator of the TRPV4 contractile effect.

TRPV4 is not activated by PIEZO1 In cultured human umbilical vein endothelial cells, PIEZO1 activation leads to downstream TRPV4 activation [42]. We tested if GSK2193874, the TRPV4

antagonist, affects responses to Yoda1, the PIEZO1 agonist. Yoda1-evoked relaxation is unaffected by GSK2193874 (Figure 5a). Similarly, GSK2193874 lacks effect on relaxation caused by Yoda2 (Figure 5b). Yoda2 is a chemical analogue of Yoda1 with improved agonist and physical and chemical properties that enables the construction of more complete concentration-response curves and therefore EC_{50} determination [36]. SC-560, the COX1 inhibitor and inhibitor of the TRPV4 response (Figure 4a), also lacks effect on the Yoda1 response (Figure 5c). The data suggest that TRPV4 and arachidonic acid metabolites do not contribute to the PIEZO1 effect on portal vein contractile tone.

Predominance of PIEZO1 in mechanical and osmotic strain The portal vein experiences mechanical and osmotic variations due to events such as postprandial hyper-perfusion of the liver, physical exercise-dependent hypo-perfusion of the liver and the drinking of water. To test if PIEZO1 and TRPV4 responses are affected by such events, we generated conditions in the myograph to increase vessel wall tension or lower osmolality. PE increases tension in the portal vein from about 0.8 to 2.2 mN (e.g., Figure 1a, d). To achieve similar tension mechanically (without applying PE), we increased basal stretch by increasing the separation between the wires in the lumen, raising basal tension from 0.8 ± 0.4 mN (Normal) to 2.2 ± 0.2 mN (Hyper-stretch). These tensions are approximately equivalent to those expected in response to ~6 mmHg (normal pressure) [56] and ~15 mmHg (high pressure similar to that of portal hypertension)[57]. Acute drinking of 1 mL of water by mice lowers the osmolality of portal vein perfusate by about 25 $mOsm.kg^{-1}$ [11]. The standard recording solution in our portal vein experiments was 282 $mOsm.kg^{-1}$, so we lowered it to 255 $mOsm.kg^{-1}$ (by reducing the NaCl concentration) to generate lower osmolality (Hypo-tonicity).

Hyper-stretch alone may slightly increase Yoda1- and Yoda2-evoked (PIEZO1) relaxations, hypo-tonicity has no effect but the combination significantly amplifies the relaxation (Figure 6a, SI Figure S5). As in normal conditions (Figure 5a, b), the TRPV4 antagonist (GSK2193874) does not affect Yoda1 responses in the hyper-stretch and hypo-tonicity condition (Figure 6b, SI Figure S6). Hyper-stretch or hypo-tonicity strongly suppress GSK1016790A-evoked (TRPV4) contractions (Figure 7a *cf* Figure 2a). A reason for such suppression could be that TRPV4 channels are already activated by the hyper-stretch or hypo-tonicity, but this is not the case because the TRPV4 antagonist, GSK2193874, does not affect tone in either condition (in the absence of GSK1016790A) (Figure 7b-e). Responses to 60 mM K^+, PE or ACh are not affected by hyper-stretch or hypo-tonicity (SI Figure S7). The data suggest that hyper-stretch and hypo-tonicity cause a switch away from functional relevance of TRPV4 to predominance of PIEZO1.

Discussion and Conclusions

The results of this study suggest that PIEZO1 and TRPV4 are functionally relevant in portal vein contractile tone and have opposing independent effects of promoting relaxation and contraction respectively, as summarised in the Graphical Abstract. Both effects are endothelium-dependent but via different mechanisms, which are nitric oxide synthase for PIEZO1 and arachidonic acid metabolism for TRPV4. In mechanical and osmotic stress, the PIEZO1 effect increases and the TRPV4 effect decreases, leading to predominance of PIEZO1. The different functional effects are surprising for channels that are similarly Ca^{2+} permeable and non-selectively permeable to cations. A potential explanation is functional separation, such as compartmentalization, of the channels in endothelium. The suggestion from studies of human umbilical vein endothelial cells that TRPV4 is downstream of PIEZO1 and therefore coupled [42] is not relevant to portal vein contraction as TRPV4 inhibition does not affect PIEZO1 agonist responses. In conditions of mechanical and osmotic stress, the PIEZO1 relaxant effect is amplified and the TRPV4 contractile effect suppressed, leading to predominance of PIEZO1 and greater potential for portal vein dilation and increased portal blood flow to the liver.

The presence of PIEZO1 in endothelium and its mediation of nitric oxide synthase activation and vessel relaxation is consistent with prior work showing that PIEZO1 agonism causes endothelial nitric oxide synthase (NOS3) phosphorylation, nitric oxide production, stabilization of NOS3 and nitric oxide synthase-dependent relaxation in intact artery, vein and microvasculature [23,24,27,28,58,59]. PIEZO1 channels do however create a dichotomy for endothelium because they are Ca^{2+} permeable non-selective cation channels, the activation of which causes both intracellular Ca^{2+} elevation and membrane depolarisation [43]. Ca^{2+} elevation is associated with NOS3 activation but depolarisation

436 opposes endothelial hyperpolarisation, which is a relaxant mechanism often referred to as
437 endothelium-derived hyperpolarisation (EDH) [60]. Therefore, PIEZO1 can cause contraction by
438 opposing EDH [43]. The relative significance of PIEZO1's pro-NOS3 (relaxant) and anti-EDH
439 (contractile) effects is likely to vary depending on the blood vessel type and context [43]. The anti-EDH
440 mechanism may have little or no relevance to contractile function if gap junctions between
441 endothelial cells and underlying smooth muscle cells are low in number, non-functional or absent,
442 as gap junctions transmit EDH to smooth muscle cells for functional effect. In portal vein, gap
443 junctions are sparse and evident only between smooth muscle cells [4].
444
445 TRPV4 mediates endothelium-dependent contraction of aorta in normotensive and hypertensive
446 animals, also via COX mechanisms, showing increased impact with ageing [61-64]. There is evidence
447 of the dichotomy here too, with TRPV4-mediated relaxant effects occurring, for example in coronary
448 arterioles [65]. The relationships of such effects to PIEZO1, other than what we show here for portal
449 vein, are unknown.
450
451 Amplification of the PIEZO1 response by hyper-stretch and hypo-tonicity is consistent with prior
452 knowledge of PIEZO1 because both factors amplify PIEZO1 activity [18,21,22]. Yoda1 effects synergize
453 with effects of mechanical force [66]. The suppression of TRPV4 responses by these factors may be
454 due to effects indirectly associated with TRPV4 rather than effects directly on TRPV4 itself. The
455 switch to dominance of PIEZO1 suggests that there is likely to be increased portal vein relaxation in
456 these conditions. In this study, the portal vein was investigated in isolation; as such, the impact of
457 blood flowing through the vessel, as well as endocrine and neurogenic effects may alter the response
458 to hypo-tonicity *in vitro* and in the *in vivo* hepatic circulation [7,8].
459
460 The TRPV4 antagonist, GSK2193874, is a good tool for exploring TRPV4 biology *in vitro* and *in*
461 *vivo*[46]. It has cross-species potency at TRPV4, efficacy against TRPV4 channels that are activated
462 by diverse stimuli and apparent selectivity for TRPV4[46]. In a rat model of heart failure, GSK2193874
463 prevents and reverses pulmonary oedema, acting only at pathological pulmonary venous pressure[67].
464 An analogue of GSK2193874 shows further benefit in pulmonary oedema of congestive heart
465 failure[68]. Small-molecules of this type therefore have therapeutic potential. These data and our new
466 findings suggest that it would be worth exploring TRPV4 in other conditions of high pressure such
467 as portal hypertension. We found TRPV4 to be less active in acute mechanical and osmotic stress
468 but its roles in portal pathologies are currently unknown. The strong effect of celecoxib against
469 TRPV4-mediated contraction in the portal vein should be considered in the context of evidence of its
470 potential value in the treatment of portal hypertension and liver cirrhosis[69-71]. Inhibition of TRPV4
471 activation could be a contributor to celecoxib's effects in these situations.
472
473 The mechanisms by which effects of Yoda1 synergise those of mechanical and osmotic stress are
474 unknown. It would be helpful to know the mechanisms because we might then be better informed
475 about the contexts in which PIEZO1 agonism is likely to be most effective, which we speculate might
476 be in ageing and diseases such as hypertension. Results of *in vitro* PIEZO1 overexpression studies
477 have suggested synergism at the level of the PIEZO1 channel itself[66], potentially with Yoda1 acting
478 as a "molecular wedge" that lowers PIEZO1 sensitivity to mechanical force[72]. PIEZO1 may however
479 achieve mechanical sensitivity through multiple mechanisms that include its interaction with
480 cytoskeletal and extracellular matrix proteins and cell-cell junction proteins such as adhesion
481 molecules[18,45,73,74]. Therefore, multiple factors may explain Yoda1's increased effect in mechanical
482 and osmotic stress. Specific investigations of this in portal pathologies such as portal hypertension
483 would be particularly valuable. At present, we lack information on what happens to the expression
484 or function of PIEZO1 or TRPV4 in such pathologies.
485
486 In conclusion, we reveal opposing independent roles of PIEZO1 and TRPV4 in the regulation of
487 portal tone and suggest predominance of PIEZO1 in conditions of mechanical and osmotic stress.
488 PIEZO1 is likely therefore to have particular significance in controlling first-pass metabolism,
489 detoxification of blood contents and gluconeogenesis. While PIEZO1 may be capable of signalling
490 to TRPV4 in other endothelial situations, this is not relevant to portal contraction. The channels are
491 remarkably separate despite sharing endothelial dependence. In future, it will be important to
492 determine the roles of PIEZO1 and PIEZO1 agonism in human hepatic vascul

ature, especially in conditions of increased pressure and lower osmolality, as can occur in liver disease, liver surgery and excessive drinking of water. Such studies could lead to important new opportunities for modulating liver perfusion and improving liver regeneration after disease-related injury or surgery.

Author contributions

N.E. planned and coordinated experimental work, performed experiments, did data analysis, prepared figures and co-wrote the paper. N.Y. and G.P. provided technical assistance. E.C.B. performed the microscopy experiments. T.S.F. and L.L. bred and maintained genetically engineered mice according to Home Office Licence requirements. T.S.F. coordinated genotyping and performed TAM injections. L.L. perfusion-fixed mice. C.R. performed chemical synthesis and validation. N.H. and A.A. designed and generated PIEZO1^{HA} mice. L.C.M., R.M.C. and K.R.P. provided intellectual input. R.F. led the chemical synthesis and generation funds for the chemistry. D.J.B. initiated the project, generated research funds and ideas, led and coordinated the project, interpreted data and co-wrote the paper.

References

1. Carneiro C, Brito J, Bilreiro C, et al. All about portal vein: a pictorial display to anatomy, variants and physiopathology. *Insights Imaging.* 2019;10(1):38.
2. Perry RJ, Zhang D, Guerra MT, et al. Glucagon stimulates gluconeogenesis by INSP3R1-mediated hepatic lipolysis. *Nature.* 2020;579(7798):279-283.
3. Schoen JM, Wang HH, Minuk GY, Lautt WW. Shear stress-induced nitric oxide release triggers the liver regeneration cascade. *Nitric Oxide.* 2001;5(5):453-464.
4. Takahashi S, Hitomi J, Satoh Y, Takahashi T, Asakura H, Ushiki T. Fine structure of the mouse portal vein in relation to its peristaltic movement. *Arch Histol Cytol.* 2002;65(1):71-82.
5. Thievent A, Connat JL. Cytoskeletal features in longitudinal and circular smooth muscles during development of the rat portal vein. *Cell Tissue Res.* 1995;279(1):199-208.
6. Mathison R. Actions of neurotransmitters and peptides on longitudinal and circular muscle of the rat portal vein. *J Pharm Pharmacol.* 1983;35(1):34-37.
7. Mai TH, Garland EM, Diedrich A, Robertson D. Hepatic and renal mechanisms underlying the osmopressor response. *Auton Neurosci.* 2017;203:58-66.
8. Tsai SH, Lin JY, Lin YC, Liu YP, Tung CS. Portal vein innervation underlying the pressor effect of water ingestion with and without cold stress. *Chin J Physiol.* 2020;63(2):53-59.
9. Albinsson S, Nordstrom I, Sward K, Hellstrand P. Differential dependence of stretch and shear stress signaling on caveolin-1 in the vascular wall. *Am J Physiol Cell Physiol.* 2008;294(1):C271-279.
10. Teichgraber UK, Gebel M, Benter T, Manns MP. Effect of respiration, exercise, and food intake on hepatic vein circulation. *J Ultrasound Med.* 1997;16(8):549-554.
11. Lechner SG, Markworth S, Poole K, et al. The molecular and cellular identity of peripheral osmoreceptors. *Neuron.* 2011;69(2):332-344.
12. George SM, Eckert LM, Martin DR, Giddens DP. Hemodynamics in Normal and Diseased Livers: Application of Image-Based Computational Models. *Cardiovasc Eng Technol.* 2015;6(1):80-91.
13. Vuppalanchi R, Noureddin M, Alkhouri N, Sanyal AJ. Therapeutic pipeline in nonalcoholic steatohepatitis. *Nat Rev Gastroenterol Hepatol.* 2021;18(6):373-392.
14. Asencio JM, Vaquero J, Olmedilla L, Garcia Sabrido JL. "Small-for-flow" syndrome: shifting the "size" paradigm. *Med Hypotheses.* 2013;80(5):573-577.
15. Fritzsche M. Thinking multi-scale to advance mechanobiology. *Commun Biol.* 2020;3(1):469.
16. Coste B, Mathur J, Schmidt M, et al. Piezo1 and Piezo2 are essential components of distinct mechanically activated cation channels. *Science.* 2010;330(6000):55-60.
17. Murthy SE, Dubin AE, Patapoutian A. Piezos thrive under pressure: mechanically activated ion channels in health and disease. *Nat Rev Mol Cell Biol.* 2017;18(12):771-783.
18. Jiang Y, Yang X, Jiang J, Xiao B. Structural Designs and Mechanogating Mechanisms of the Mechanosensitive Piezo Channels. *Trends Biochem Sci.* 2021;46(6):472-488.

19. Guo YR, MacKinnon R. Structure-based membrane dome mechanism for Piezo mechanosensitivity. *Elife.* 2017;6.
20. Wang L, Zhou H, Zhang M, et al. Structure and mechanogating of the mammalian tactile channel PIEZO2. *Nature.* 2019;573(7773):225-229.
21. Gottlieb PA, Bae C, Sachs F. Gating the mechanical channel Piezo1: a comparison between whole-cell and patch recording. *Channels (Austin).* 2012;6(4):282-289.
22. Zhao T, Parmisano S, Soroureddin Z, et al. Mechanosensitive cation currents through TRPC6 and Piezo1 channels in human pulmonary arterial endothelial cells. *Am J Physiol Cell Physiol.* 2022;323(4):C959-C973.
23. Beech DJ, Kalli AC. Force Sensing by Piezo Channels in Cardiovascular Health and Disease. *Arterioscler Thromb Vasc Biol.* 2019;39(11):2228-2239.
24. Li J, Hou B, Tumova S, et al. Piezo1 integration of vascular architecture with physiological force. *Nature.* 2014;515(7526):279-282.
25. Rode B, Shi J, Endesh N, et al. Piezo1 channels sense whole body physical activity to reset cardiovascular homeostasis and enhance performance. *Nat Commun.* 2017;8(1):350.
26. Shi J, Hyman AJ, De Vecchis D, et al. Sphingomyelinase Disables Inactivation in Endogenous PIEZO1 Channels. *Cell Rep.* 2020;33(1):108225.
27. Wang S, Chennupati R, Kaur H, Iring A, Wettschureck N, Offermanns S. Endothelial cation channel PIEZO1 controls blood pressure by mediating flow-induced ATP release. *J Clin Invest.* 2016;126(12):4527-4536.
28. Bartoli F, Debant M, Chuntharpursat-Bon E, et al. Endothelial Piezo1 sustains muscle capillary density and contributes to physical activity. *J Clin Invest.* 2022;132(5).
29. Kang H, Hong Z, Zhong M, et al. Piezo1 mediates angiogenesis through activation of MT1-MMP signaling. *Am J Physiol Cell Physiol.* 2019;316(1):C92-C103.
30. Friedrich EE, Hong Z, Xiong S, et al. Endothelial cell Piezo1 mediates pressure-induced lung vascular hyperpermeability via disruption of adherens junctions. *Proc Natl Acad Sci U S A.* 2019;116(26):12980-12985.
31. Wang S, Wang B, Shi Y, et al. Mechanosensation by endothelial PIEZO1 is required for leukocyte diapedesis. *Blood.* 2022;140(3):171-183.
32. Retailleau K, Duprat F, Arhatte M, et al. Piezo1 in Smooth Muscle Cells Is Involved in Hypertension-Dependent Arterial Remodeling. *Cell Rep.* 2015;13(6):1161-1171.
33. Zeng WZ, Marshall KL, Min S, et al. PIEZOs mediate neuronal sensing of blood pressure and the baroreceptor reflex. *Science.* 2018;362(6413):464-467.
34. Caolo V, Debant M, Endesh N, et al. Shear stress activates ADAM10 sheddase to regulate Notch1 via the Piezo1 force sensor in endothelial cells. *Elife.* 2020;9.
35. Hilscher MB, Sehrawat T, Arab JP, et al. Mechanical Stretch Increases Expression of CXCL1 in Liver Sinusoidal Endothelial Cells to Recruit Neutrophils, Generate Sinusoidal Microthombi, and Promote Portal Hypertension. *Gastroenterology.* 2019;157(1):193-209 e199.
36. Parsonage G, Cuthbertson K, Endesh N, et al. Improved PIEZO1 agonism through 4-benzoic acid modification of Yoda1. *Br J Pharmacol.* 2022.
37. White JP, Cibelli M, Urban L, Nilius B, McGeown JG, Nagy I. TRPV4: Molecular Conductor of a Diverse Orchestra. *Physiol Rev.* 2016;96(3):911-973.
38. Kohler R, Heyken WT, Heinau P, et al. Evidence for a functional role of endothelial transient receptor potential V4 in shear stress-induced vasodilatation. *Arterioscler Thromb Vasc Biol.* 2006;26(7):1495-1502.
39. Mendoza SA, Fang J, Gutterman DD, et al. TRPV4-mediated endothelial Ca2+ influx and vasodilation in response to shear stress. *American Journal of Physiology-Heart and Circulatory Physiology.* 2010;298(2):H466-H476.
40. Liu L, Guo M, Lv X, et al. Role of Transient Receptor Potential Vanilloid 4 in Vascular Function. *Front Mol Biosci.* 2021;8:677661.
41. Hyman AJ, Tumova S, Beech DJ. Piezo1 Channels in Vascular Development and the Sensing of Shear Stress. *Curr Top Membr.* 2017;79:37-57.
42. Swain SM, Liddle RA. Piezo1 acts upstream of TRPV4 to induce pathological changes in endothelial cells due to shear stress. *Journal of Biological Chemistry.* 2021;296.

43. Rode B, Shi J, Endesh N, et al. Piezo1 channels sense whole body physical activity to reset cardiovascular homeostasis and enhance performance. *Nature communications.* 2017;8(1):1-11.
44. Kaneko T. Genome Editing in Mouse and Rat by Electroporation. *Methods in molecular biology.* 2017;1630:81-89.
45. Chuntharpursat-Bon E, Povstyan OV, Ludlow MJ, et al. PIEZO1 and PECAM1 interact at cell-cell junctions and partner in endothelial force sensing. *Commun Biol.* 2023;6(1):358.
46. Cheung M, Bao W, Behm DJ, et al. Discovery of GSK2193874: An Orally Active, Potent, and Selective Blocker of Transient Receptor Potential Vanilloid 4. *ACS Med Chem Lett.* 2017;8(5):549-554.
47. Thorneloe KS, Sulpizio AC, Lin Z, et al. N-((1S)-1-{[4-((2S)-2-{[(2, 4-dichlorophenyl) sulfonyl] amino}-3-hydroxypropanoyl)-1-piperazinyl] carbonyl}-3-methylbutyl)-1-benzothiophene-2-carboxamide (GSK1016790A), a novel and potent transient receptor potential vanilloid 4 channel agonist induces urinary bladder contraction and hyperactivity: Part I. *Journal of Pharmacology and Experimental Therapeutics.* 2008;326(2):432-442.
48. Vanhoutte PM, Zhao Y, Xu A, Leung SW. Thirty Years of Saying NO: Sources, Fate, Actions, and Misfortunes of the Endothelium-Derived Vasodilator Mediator. *Circ Res.* 2016;119(2):375-396.
49. Shimamura K, Kimura S, Zhou M, et al. Evidence for the involvement of the cyclooxygenase-metabolic pathway in diclofenac-induced inhibition of spontaneous contraction of rat portal vein smooth muscle cells. *J Smooth Muscle Res.* 2005;41(4):195-206.
50. Feletou M, Huang Y, Vanhoutte PM. Endothelium-mediated control of vascular tone: COX-1 and COX-2 products. *Br J Pharmacol.* 2011;164(3):894-912.
51. Smith CJ, Zhang Y, Koboldt CM, et al. Pharmacological analysis of cyclooxygenase-1 in inflammation. *Proc Natl Acad Sci U S A.* 1998;95(22):13313-13318.
52. Penning TD, Talley JJ, Bertenshaw SR, et al. Synthesis and biological evaluation of the 1,5-diarylpyrazole class of cyclooxygenase-2 inhibitors: identification of 4-[5-(4-methylphenyl)-3-(trifluoromethyl)-1H-pyrazol-1-yl]benze nesulfonamide (SC-58635, celecoxib). *J Med Chem.* 1997;40(9):1347-1365.
53. Balsinde J, Balboa MA, Insel PA, Dennis EA. Regulation and inhibition of phospholipase A2. *Annu Rev Pharmacol Toxicol.* 1999;39:175-189.
54. Alexander SP, Fabbro D, Kelly E, et al. THE CONCISE GUIDE TO PHARMACOLOGY 2021/22: Enzymes. *Br J Pharmacol.* 2021;178 Suppl 1:S313-S411.
55. Queck A, Thomas D, Jansen C, et al. Pathophysiological role of prostanoids in coagulation of the portal venous system in liver cirrhosis. *PLoS One.* 2019;14(10):e0222840.
56. Xie C, Wei W, Zhang T, Dirsch O, Dahmen U. Monitoring of systemic and hepatic hemodynamic parameters in mice. *JoVE (Journal of Visualized Experiments).* 2014(92):e51955.
57. Fernandez M, Vizzutti F, Garcia-Pagan JC, Rodes J, Bosch J. Anti-VEGF receptor-2 monoclonal antibody prevents portal-systemic collateral vessel formation in portal hypertensive mice. *Gastroenterology.* 2004;126(3):886-894.
58. Evans EL, Cuthbertson K, Endesh N, et al. Yoda1 analogue (Dooku1) which antagonizes Yoda1-evoked activation of Piezo1 and aortic relaxation. *Br J Pharmacol.* 2018;175(10):1744-1759.
59. Jin YJ, Chennupati R, Li R, et al. Protein kinase N2 mediates flow-induced endothelial NOS activation and vascular tone regulation. *J Clin Invest.* 2021;131(21).
60. Garland CJ, Dora KA. EDH: endothelium-dependent hyperpolarization and microvascular signalling. *Acta Physiol (Oxf).* 2017;219(1):152-161.
61. Wong MS-K, Vanhoutte PM. COX-mediated endothelium-dependent contractions: from the past to recent discoveries. *Acta Pharmacologica Sinica.* 2010;31(9):1095-1102.
62. Wong SL, Leung FP, Lau CW, et al. Cyclooxygenase-2–derived prostaglandin F2α mediates endothelium-dependent contractions in the aortae of hamsters with increased impact during aging. *Circulation research.* 2009;104(2):228-235.
63. Saifeddine M, El-Daly M, Mihara K, et al. GPCR-mediated EGF receptor transactivation regulates TRPV 4 action in the vasculature. *British Journal of Pharmacology.* 2015;172(10):2493-2506.

64. Zhang P, Sun C, Li H, et al. TRPV4 (transient receptor potential vanilloid 4) mediates endothelium-dependent contractions in the aortas of hypertensive mice. *Hypertension.* 2018;71(1):134-142.
65. Zheng X, Zinkevich NS, Gebremedhin D, et al. Arachidonic Acid–Induced Dilation in Human Coronary Arterioles: Convergence of Signaling Mechanisms on Endothelial TRPV 4-Mediated Ca2+ Entry. *Journal of the American Heart Association.* 2013;2(3):e000080.
66. Syeda R, Xu J, Dubin AE, et al. Chemical activation of the mechanotransduction channel Piezo1. *Elife.* 2015;4.
67. Thorneloe KS, Cheung M, Bao W, et al. An orally active TRPV4 channel blocker prevents and resolves pulmonary edema induced by heart failure. *Sci Transl Med.* 2012;4(159):159ra148.
68. Brooks CA, Barton LS, Behm DJ, et al. Discovery of GSK2798745: A Clinical Candidate for Inhibition of Transient Receptor Potential Vanilloid 4 (TRPV4). *ACS Med Chem Lett.* 2019;10(8):1228-1233.
69. Gao JH, Wen SL, Yang WJ, et al. Celecoxib ameliorates portal hypertension of the cirrhotic rats through the dual inhibitory effects on the intrahepatic fibrosis and angiogenesis. *PLoS One.* 2013;8(7):e69309.
70. Tai Y, Zhao C, Zhang L, et al. Celecoxib reduces hepatic vascular resistance in portal hypertension by amelioration of endothelial oxidative stress. *J Cell Mol Med.* 2021;25(22):10389-10402.
71. Tang S, Huang Z, Jiang J, et al. Celecoxib ameliorates liver cirrhosis via reducing inflammation and oxidative stress along spleen-liver axis in rats. *Life Sci.* 2021;272:119203.
72. Botello-Smith WM, Jiang W, Zhang H, et al. A mechanism for the activation of the mechanosensitive Piezo1 channel by the small molecule Yoda1. *Nat Commun.* 2019;10(1):4503.
73. Wang J, Jiang J, Yang X, Zhou G, Wang L, Xiao B. Tethering Piezo channels to the actin cytoskeleton for mechanogating via the cadherin-beta-catenin mechanotransduction complex. *Cell Rep.* 2022;38(6):110342.
74. Lai A, Thurgood P, Cox CD, et al. Piezo1 Response to Shear Stress Is Controlled by the Components of the Extracellular Matrix. *ACS Appl Mater Interfaces.* 2022;14(36):40559-40568.

Figure Legends

Figure 1: PIEZO1 agonism causes nitric oxide synthase (NOS)-dependent relaxation Control and gene-modified mouse portal vein tension data (endothelium intact). (**a**) Example tension trace obtained from a control mouse contracted with 10 μM phenylephrine (PE) and then exposed to 0.1, 0.3, 1, 3 and 10 μM Yoda1 (PIEZO1 agonist) as indicated by the 5 dots. (**b**) As for (**a**) but from a PIEZO1$^{\Delta EC}$ mouse. (**c**) Summary data for Yoda1 responses of the types shown in (**a**, **b**) in n=8 control mice (grey) and n=9 PIEZO1$^{\Delta EC}$ mice (blue). (**d**) As for (**a**) but with a second set of concentration-response data for Yoda1 in the presence of 100 μM L-NAME. At the end of the recording, 10 μM SIN-1 (a nitric oxide donor) was applied to show response to exogenous nitric oxide. Irregularities in the trace after the first Yoda1 applications occurred when the recording chamber was washed out 3 times (3x wash). (**e**) Summary data for n=7 experiments (i.e., from 7 mice) of the type shown in (**d**) for the vehicle control (grey) or L-NAME (blue). (**c**, **e**) Symbols and error bars are mean ± SD. Superimposed dotted lines are the underlying original data. Unpaired (**c**) and paired (**d**) t-tests for PIEZO1$^{\Delta EC}$ compared with control mouse data at the indicated Yoda1 concentration: $^{**}P < 0.01$, $^{***}P < 0.001$ and NS where there are no asterisks. n indicates the number of mice.

Figure 2: TRPV4 agonism causes contraction Control mouse portal vein tension data (endothelium intact). (**a**) Example tension trace and mean summary data for contraction induced by 1 nM GSK1016790A (TRPV4 agonist) applied twice with wash-out in between ((1) and (2)) (n=5). (**b**) Example tension trace for contraction induced by increasing concentrations of GSK1016790A (0.2, 0.4, 0.6, 0.8, 1 and 3 nM) as indicated the 6 dots, with summary data to the right (n=5). The smooth curve was fitted using the Hill Equation and indicated 50 % maximum effect (EC_{50}) at 0.7 nM. (**c**) As for (**a**) but with the second GSK1016790A application in the presence of 300 nM GSK2193874 (TRPV4 antagonist) (n=5 for the summary data). (**d**) As for (**c**) but with GSK1016790A applied after 10 μM phenylephrine (PE). (n=5 for the summary data). (**a**-**d**) Symbols and error bars are mean ± SD. Superimposed dotted lines are the underlying original data. Paired t-test: (**a** NS), (**c** $^{***}P < 0.001$), (**d** $^{***}P < 0.001$) and NS where there are no asterisks. n indicates the number of mice.

Figure 3: Endothelium-dependence of the TRPV4 response Control mouse portal vein tension data. (**a**) Typical trace with endothelial cells intact (+EC) showing responses to 10 μM phenylephrine (PE), 0.3, 1, 3 and 10 μM acetylcholine (ACh) and then, after wash out, 1 nM GSK1016790A. (**b**) Typical trace for a portal vein segment without endothelial cells (-EC). (**c**) As for (**a**, **b**): data for all experiments of this type. GSK1016790A contraction as a % of contraction evoked by 60 mM K^+ plotted against ACh relaxation as a % of the maximum relaxation (pre-PE tone). Each data point is for a segment of vein (n=39). The straight line was fitted mathematically, indicating Pearson's correlation coefficient (r) 0.85. On the right, as for the left graph but excluding the data in which there was no response to ACh (n=21). r=0.87. (**d**) For +EC, example trace (left) and summary data (right) for 1 nM GSK1016790A responses before and after incubation with 100 μM L-NAME (n=5). (**e**) As for (**d**) but using 500 nM apamin (Apa) and 100 nM charybdotoxin (ChTx) (n=5). (**f**) As for (**d, e**) but using L-NAME, Apa and ChTx (n=8). Summary data are mean ± SD. Paired t-test: (**d**-**f**) (NS). n indicates the number of mice.

Figure 4: COX and PLA_2 dependence of the TRPV4 response Control mouse portal vein tension data (endothelium intact). (**a**) Example trace (left) and summary data (right) for 1 nM GSK1016790A responses before and after incubation with 1 μM SC-560 (n=5). (**b**) Similar to (**a**) but incubated with 1 μM SC-560 and 10 μM celecoxib (n=6). (**c**) Similar to (**a**) but incubated with 10 μM bromoenol lactone (n=8). (**d**) Example trace (left) and summary data (right) for responses to increasing concentrations of prostaglandin E_2 (PGE_2) (0.1, 0.3, 1, 3, 10 and 30 μM) applied twice and indicated by 6 dots each. Summary data are for n=8 and mean ± SD. Individual data are superimposed. The two colours are for the first (1) and second (2) application of PGE_2 with wash out in between. Paired t-test: (**a** $^{*}P < 0.05$), (**b**, **c** $^{***}P < 0.001$) and NS where there are no asterisks. n indicates the number of mice.

Figure 5: PIEZO1 responses do not involve TRPV4 Control mouse portal vein tension data (endothelium intact). (**a**) Example trace (left) and summary data (right) for responses to Yoda1 (0.1,

749 0.3, 1, 3 and 10 μM, indicated by the 5 dots in the left trace) before and after incubation with 300 nM
750 GSK2193874 (TRPV4 antagonist) (n=5). (**b**) As for (**a**) but using Yoda2 instead of Yoda1 (0.1, 0.3,
751 1, 3, 10 and 30 μM) (n= 5). (**c**) As for (**a**) but using 1 μM SC-560 instead of GSK2193874 (n= 5). (**a**-
752 **c**) Summary data are mean ± SD and the individual data are superimposed. Paired t-tests: NS. n
753 indicates the number of mice.
754
755 **Figure 6: Mechanical and osmotic strain amplify PIEZO1 function** Control mouse portal vein
756 tension data (endothelium intact). (**a**) Concentration-response data for Yoda1-induced relaxation in
757 normal (open symbol, 0.8 mN tension and 282 mOsm.kg^{-1}), hyper-stretch (light purple symbol, 2.2
758 mN tension and 282 mOsm.kg^{-1}) , hypo-tonicity (dark purple symbol, 0.8 mN tension and 255
759 mOsm.kg^{-1}) and combined hyper-stretch and hypo-tonicity (blue symbol, 2.2 mN tension and 255
760 mOsm.kg^{-1}) conditions (n=5, 5, 5 and 6 respectively). The normal condition data are reproduced
761 from Figure 5a and are shown only as mean values. (**b**) In the combined hyper-stretch and hypo-
762 tonicity condition, example trace (left) and summary data (right) for responses to Yoda1 (0.1, 0.3, 1,
763 3 and 10 μM, indicated by the 5 dots on the traces) before and after incubation with 300 nM
764 GSK2193874 (TRPV4 antagonist) (n= 6). The Yoda1-only data are reproduced from (**a**) and shown
765 only as mean values. ANOVA (**a**) at the indicated Yoda1 concentration: $^{**}P < 0.01$ and $^{***}P < 0.001$
766 for hyper-stretch plus hypo-tonicity compared with normal and NS where there are no asterisks. n
767 indicates the number of mice.
768
769 **Figure 7: Mechanical and osmotic strain suppress TRPV4 function** Control mouse portal vein
770 tension data (endothelium intact). (**a**) In the hyper-stretch or hypo-tonicity condition, example traces
771 (left and middle) and summary data (right) for responses to 1 nM GSK1016790A (n=8 each). The
772 summary data are for the first (1) and second (2) GSK1016790A responses with wash-out in
773 between. The normal condition data are reproduced from Figure 2a for direct comparison. (**b**-**e**) In
774 the normal, hyper-stretch or hypo-tonicity condition, example traces and summary data for PE (10
775 μM) responses without (-) and with (+) 300 nM GSK2193874 (n=8 normal, n=5 hyper-stretch, n=5
776 hypo-tonicity). Summary data are shown as mean ± SD. ANOVA: (**a** $^{***}P < 0.001$; hyper-stretch or
777 hypo-tonicity compared with normal for (1) and (2)) and (**e** NS). n indicates the number of mice.
778

Figure 1

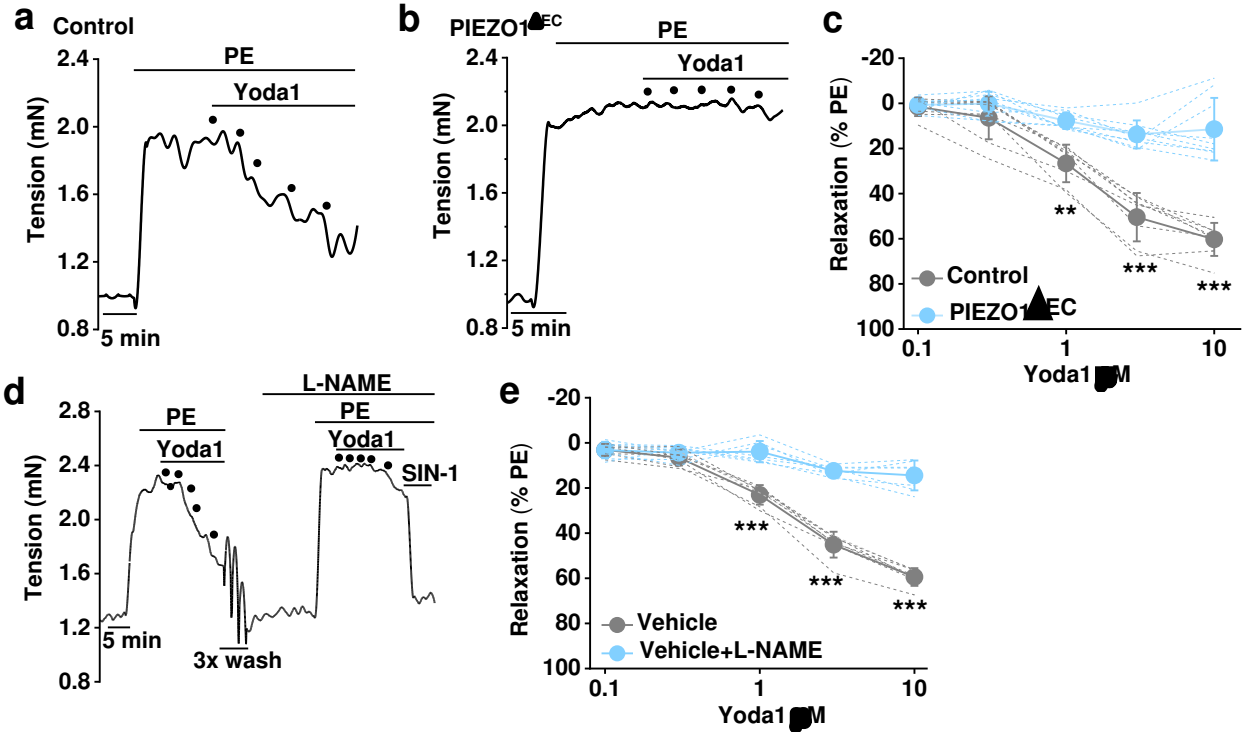
a
Control
PE
Yoda1
Tension (mN)
2.4
2.0
1.6
1.2
0.8
5 min
b
PIEZO1
EC
PE
Yoda1
Tension (mN)
5 min
c
Relaxation (% PE)
-20
0
20
40
60
80
100
**
***
***
Control
PIEZO1
EC
0.1
1
10
Yoda1
M
d
L-NAME
PE
Yoda1
PE
Yoda1
SIN-1
Tension (mN)
5 min
3x wash
e
Relaxation (% PE)
***
***
***
Vehicle
Vehicle+L-NAME
Yoda1
M

Figure 2

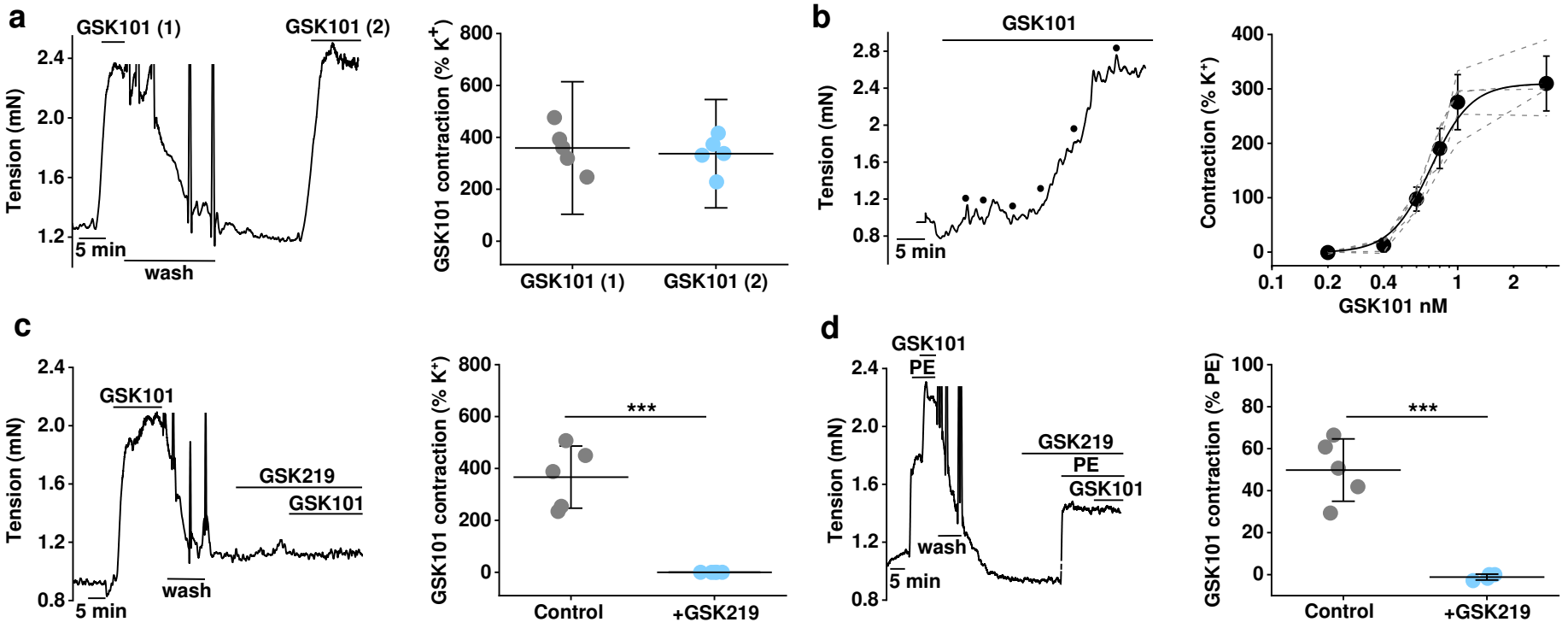
a
GSK101 (1)
GSK101 (2)
Tension (mN)
5 min
wash
GSK101 contraction (% K+)
GSK101 (1)
GSK101 (2)
b
GSK101
Tension (mN)
5 min
Contraction (% K+)
GSK101 nM
c
GSK101
GSK219
GSK101
wash
Tension (mN)
5 min
GSK101 contraction (% K+)
***
Control
+GSK219
d
GSK101
PE
GSK219
PE
GSK101
wash
Tension (mN)
5 min
GSK101 contraction (% PE)
***
Control
+GSK219

Figure 3

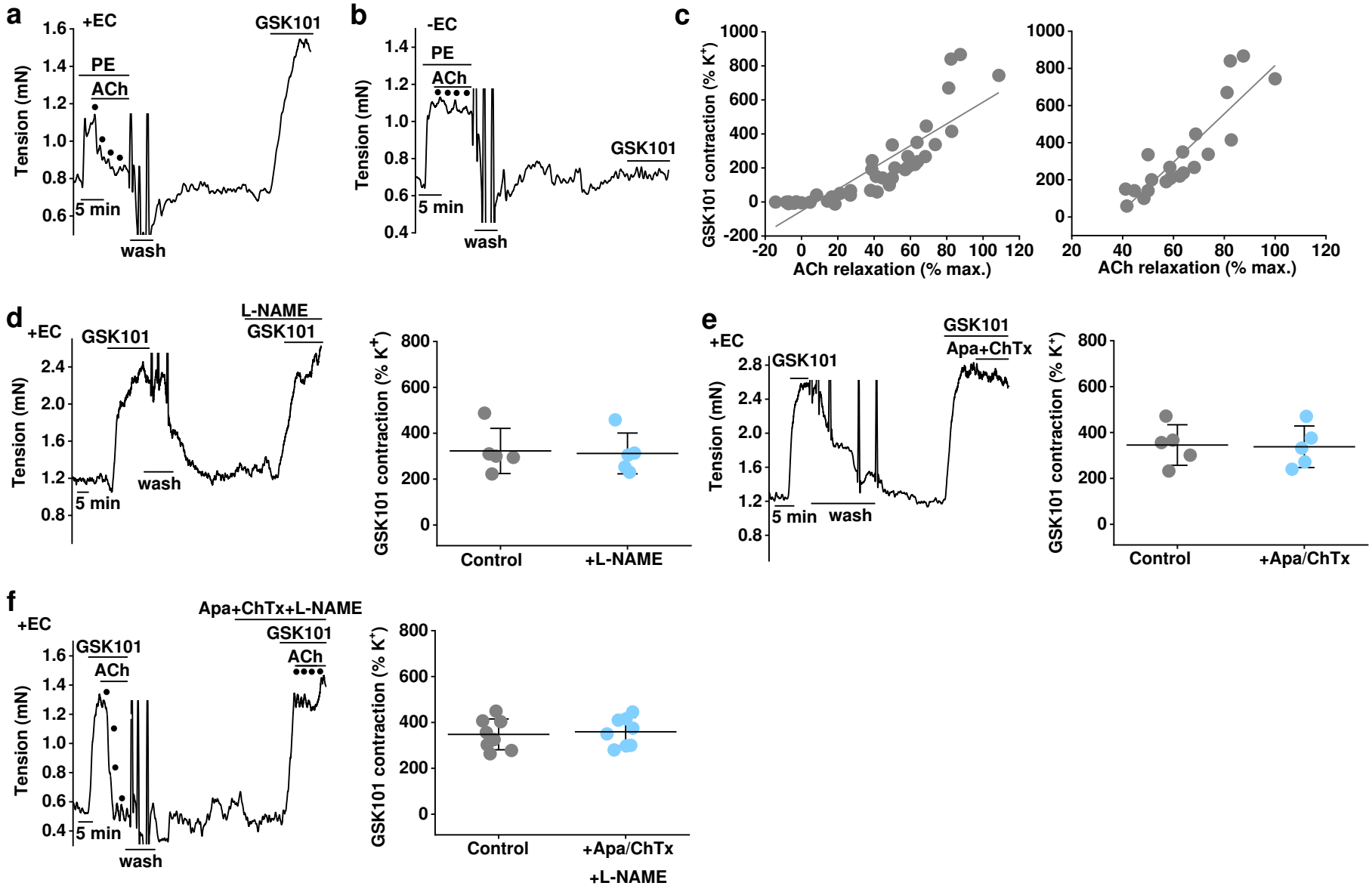
a
+EC
PE
ACh
GSK101
Tension (mN)
5 min
wash
b
-EC
PE
ACh
GSK101
Tension (mN)
5 min
wash
c
GSK101 contraction (% K+)
ACh relaxation (% max.)
ACh relaxation (% max.)
d
+EC
GSK101
L-NAME
GSK101
Tension (mN)
5 min
wash
GSK101 contraction (% K+)
Control
+L-NAME
e
+EC
GSK101
GSK101
Apa+ChTx
Tension (mN)
5 min
wash
GSK101 contraction (% K+)
Control
+Apa/ChTx
f
+EC
Apa+ChTx+L-NAME
GSK101
ACh
GSK101
ACh
Tension (mN)
5 min
wash
GSK101 contraction (% K+)
Control
+Apa/ChTx
+L-NAME

Figure 4

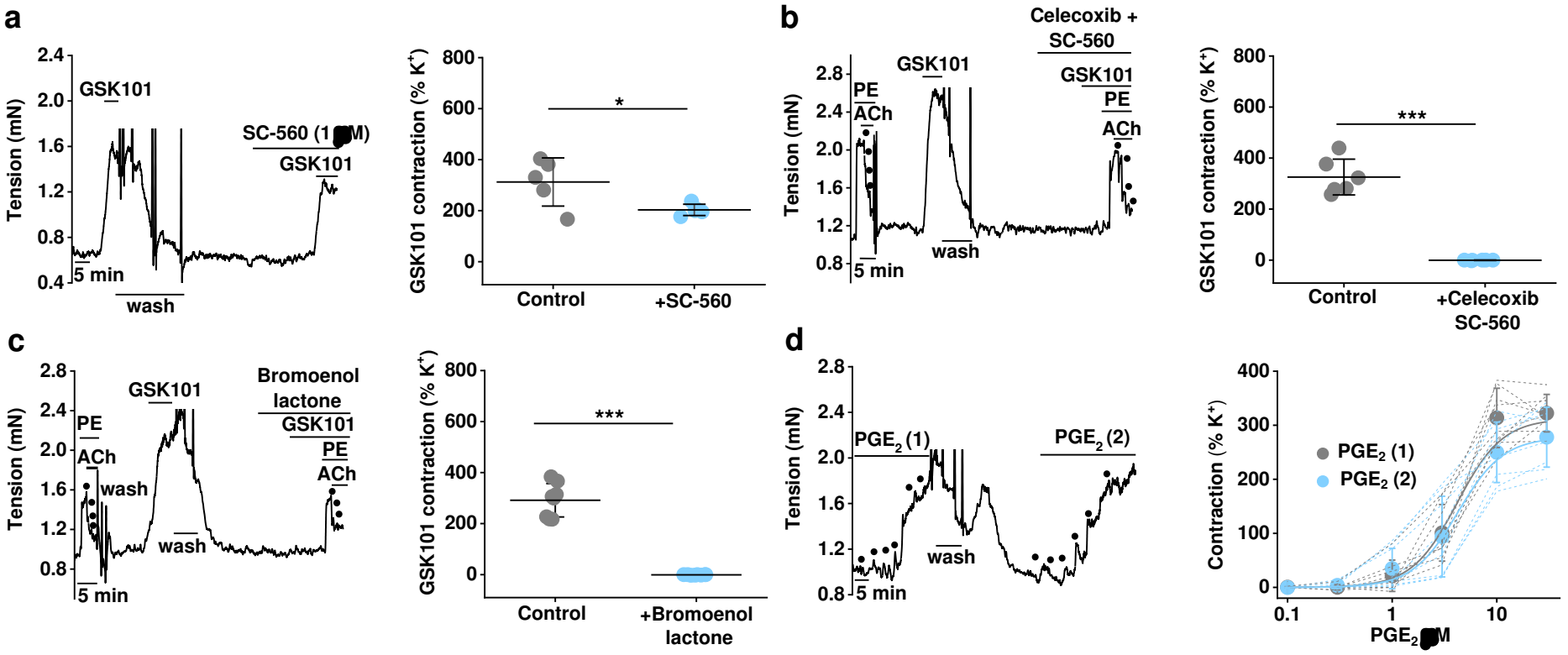
a
Tension (mN)
GSK101
SC-560 (1 μM)
GSK101
5 min
wash
GSK101 contraction (% K+)
*
Control
+SC-560
b
Celecoxib + SC-560
GSK101
PE
ACh
GSK101
PE
ACh
wash
5 min
***
Control
+Celecoxib SC-560
c
GSK101
Bromoenol lactone
PE
ACh
wash
GSK101
PE
ACh
wash
5 min
***
Control
+Bromoenol lactone
d
PGE2 (1)
PGE2 (2)
wash
5 min
Contraction (% K+)
PGE2 (1)
PGE2 (2)
PGE2 μM

Figure 5

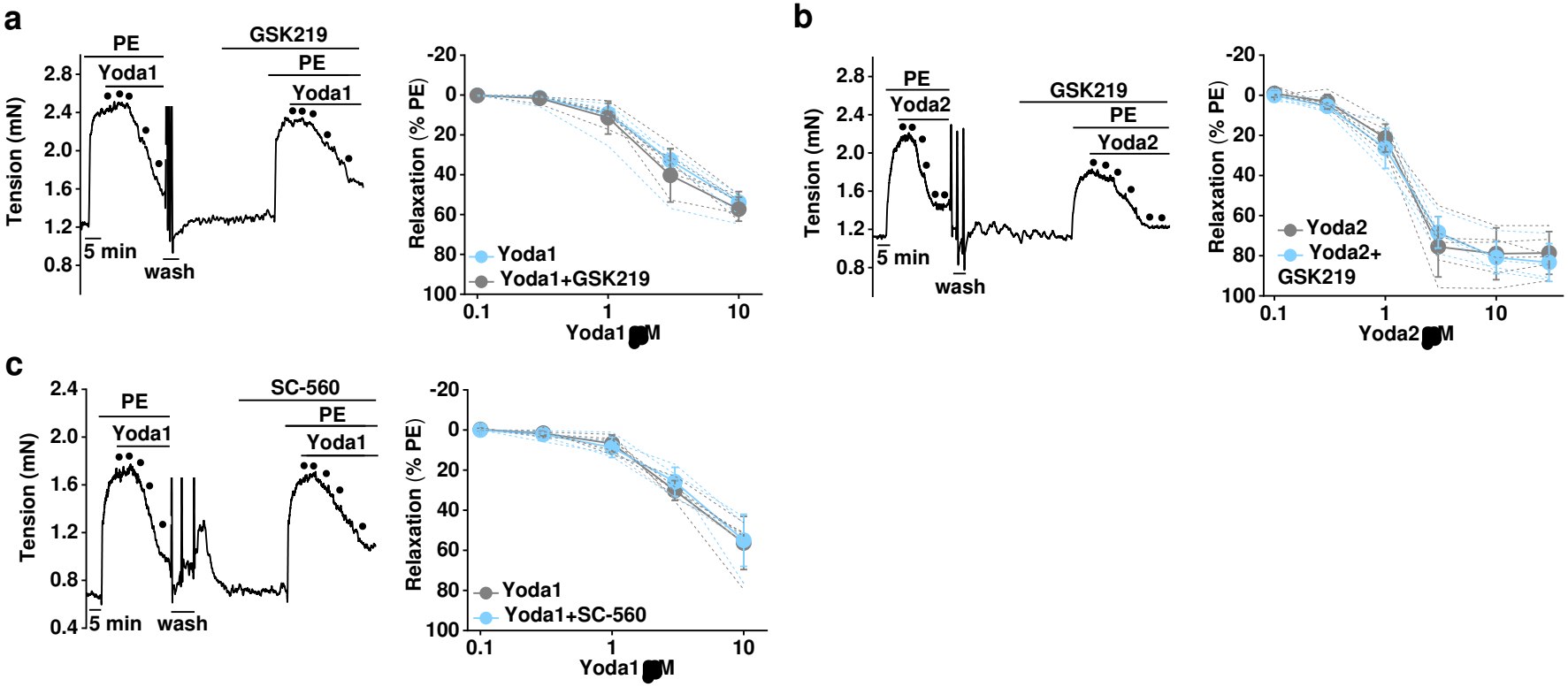
a
PE
Yoda1
GSK219
PE
Yoda1
Tension (mN)
5 min
wash
Relaxation (% PE)
Yoda1
Yoda1+GSK219
Yoda1 μM
b
PE
Yoda2
GSK219
PE
Yoda2
Tension (mN)
5 min
wash
Relaxation (% PE)
Yoda2
Yoda2+
GSK219
Yoda2 μM
c
PE
Yoda1
SC-560
PE
Yoda1
Tension (mN)
5 min
wash
Relaxation (% PE)
Yoda1
Yoda1+SC-560
Yoda1 μM

Figure 6

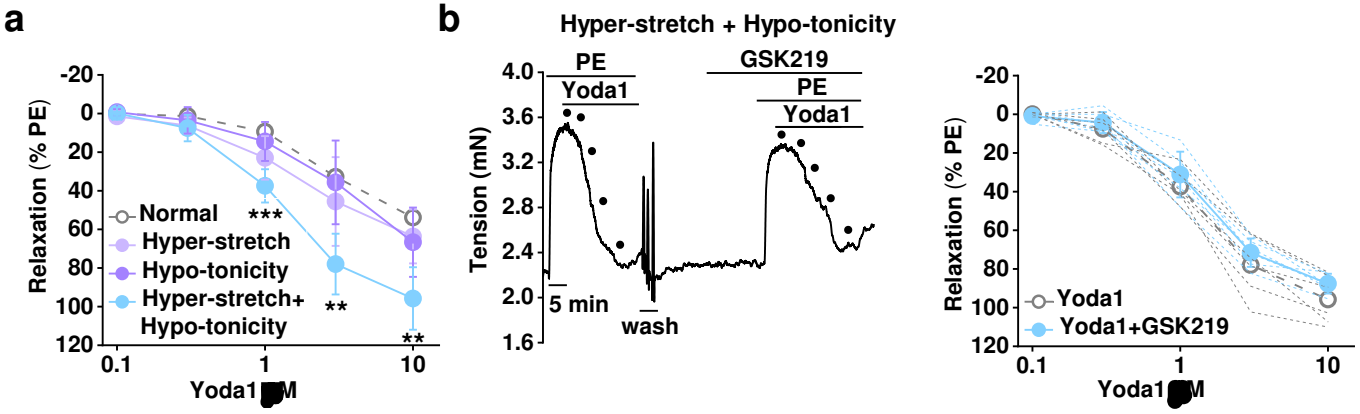
a
b
Hyper-stretch + Hypo-tonicity
PE
Yoda1
GSK219
PE
Yoda1
Relaxation (% PE)
Tension (mN)
Normal
Hyper-stretch
Hypo-tonicity
Hyper-stretch+
Hypo-tonicity
***
**
**
5 min
wash
Yoda1
Yoda1+GSK219
Yoda1 μM

Figure 7

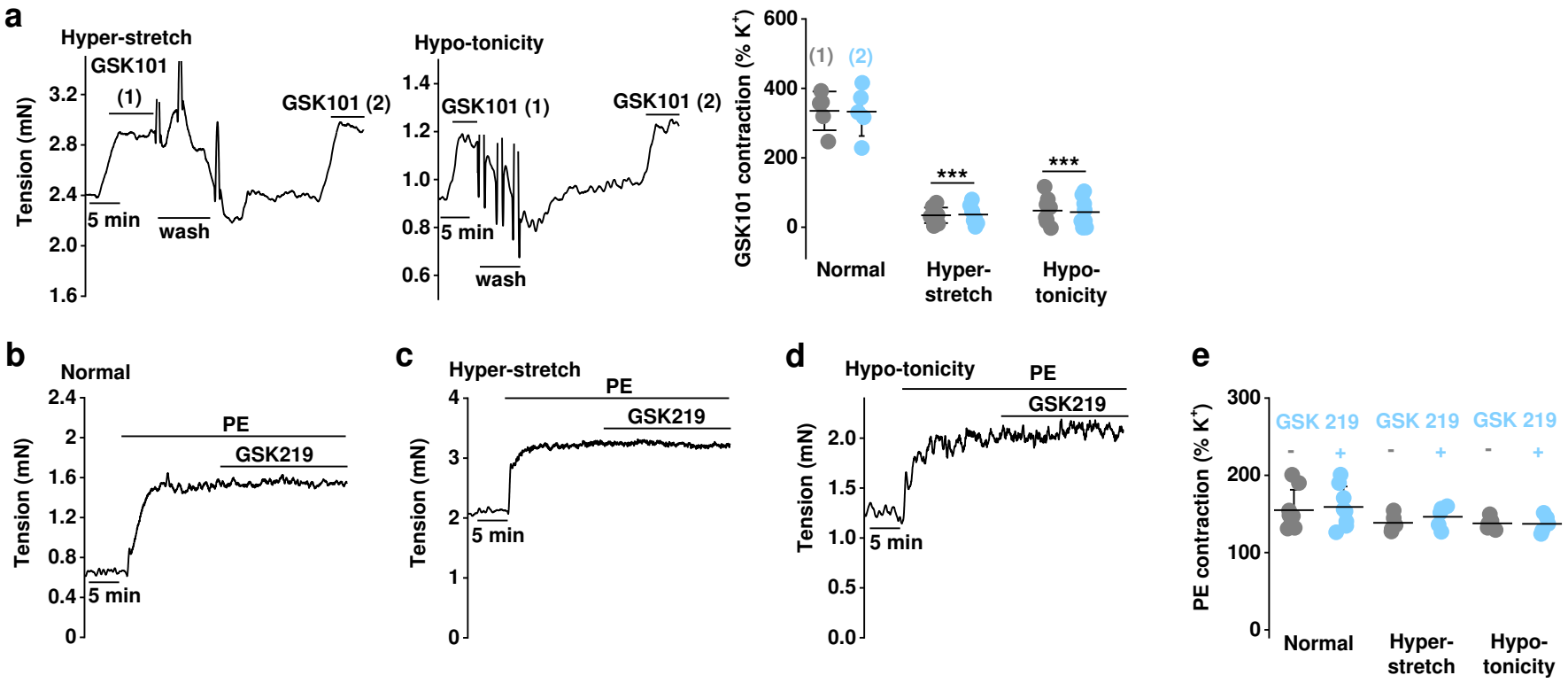
a
Hyper-stretch
GSK101
(1)
GSK101 (2)
Tension (mN)
5 min
wash
Hypo-tonicity
GSK101 (1)
GSK101 (2)
5 min
wash
GSK101 contraction (% K+)
(1)
(2)
***
***
Normal
Hyper-stretch
Hypo-tonicity
b
Normal
PE
GSK219
Tension (mN)
5 min
c
Hyper-stretch
PE
GSK219
Tension (mN)
5 min
d
Hypo-tonicity
PE
GSK219
Tension (mN)
5 min
e
GSK 219
GSK 219
GSK 219
PE contraction (% K+)
Normal
Hyper-stretch
Hypo-tonicity

SI Figure S1

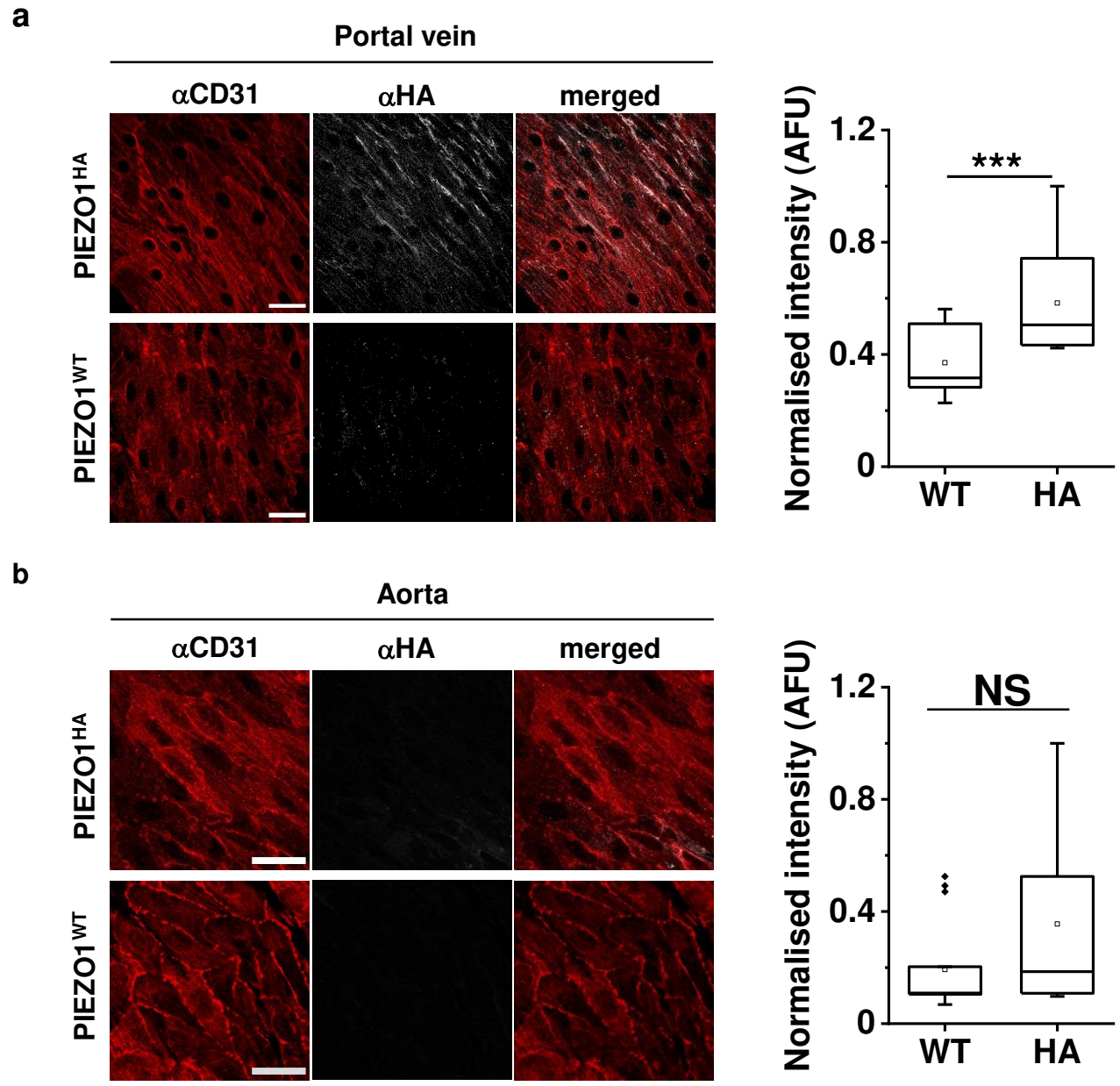
a
Portal vein
αCD31
αHA
merged
PIEZO1HA
PIEZO1WT
Normalised intensity (AFU)
1.2
0.8
0.4
0
***
WT
HA
b
Aorta
αCD31
αHA
merged
PIEZO1HA
PIEZO1WT
Normalised intensity (AFU)
1.2
0.8
0.4
0
NS
WT
HA

SI Figure S2

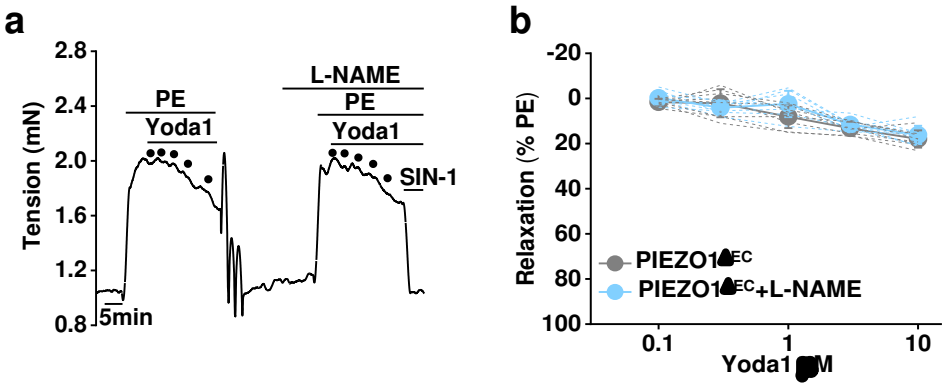
a
Tension (mN)
2.8
2.4
2.0
1.6
1.2
0.8
PE
Yoda1
L-NAME
PE
Yoda1
SIN-1
5min
b
Relaxation (% PE)
-20
0
20
40
60
80
100
PIEZO1ΔEC
PIEZO1ΔEC+L-NAME
0.1
1
10
Yoda1 μM

SI Figure S3

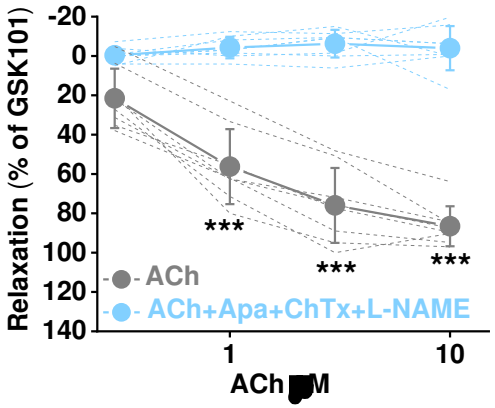
Relaxation (% of GSK101)
-20
0
20
40
60
80
100
120
140
***
***
***
ACh
ACh+Apa+ChTx+L-NAME
1
10
ACh M

SI Figure S4

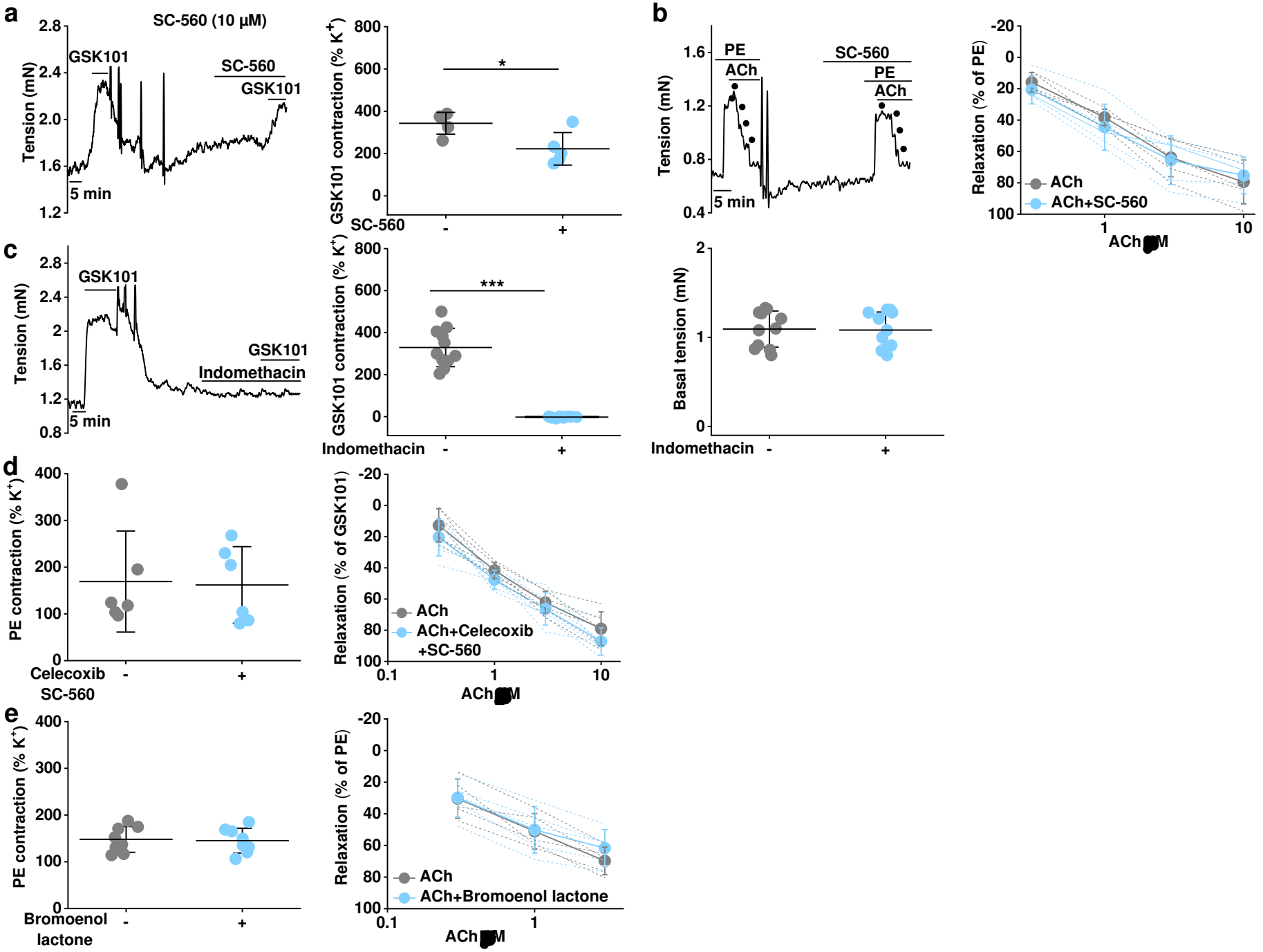
a
SC-560 (10 μM)
GSK101
SC-560
GSK101
Tension (mN)
5 min
GSK101 contraction (% K+)
SC-560
b
PE
ACh
SC-560
PE
ACh
Tension (mN)
5 min
Relaxation (% of PE)
ACh
ACh+SC-560
c
GSK101
GSK101
Indomethacin
Tension (mN)
5 min
GSK101 contraction (% K+)
Indomethacin
Basal tension (mN)
Indomethacin
d
PE contraction (% K+)
Celecoxib
SC-560
Relaxation (% of GSK101)
ACh
ACh+Celecoxib
+SC-560
e
PE contraction (% K+)
Bromoenol
lactone
Relaxation (% of PE)
ACh
ACh+Bromoenol lactone

SI Figure S5

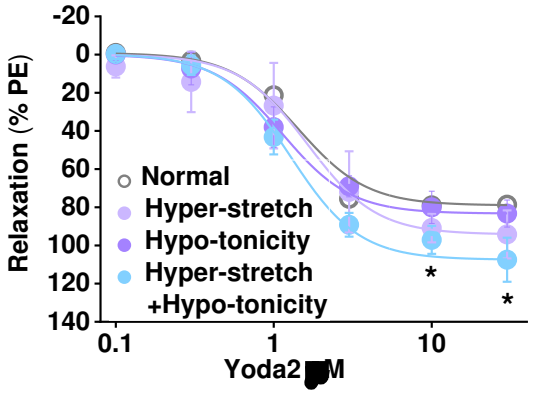
-20
0
20
40
60
80
100
120
140
Relaxation (% PE)
Normal
Hyper-stretch
Hypo-tonicity
Hyper-stretch
+Hypo-tonicity
*
*
0.1
1
10
Yoda2 M

SI Figure S6

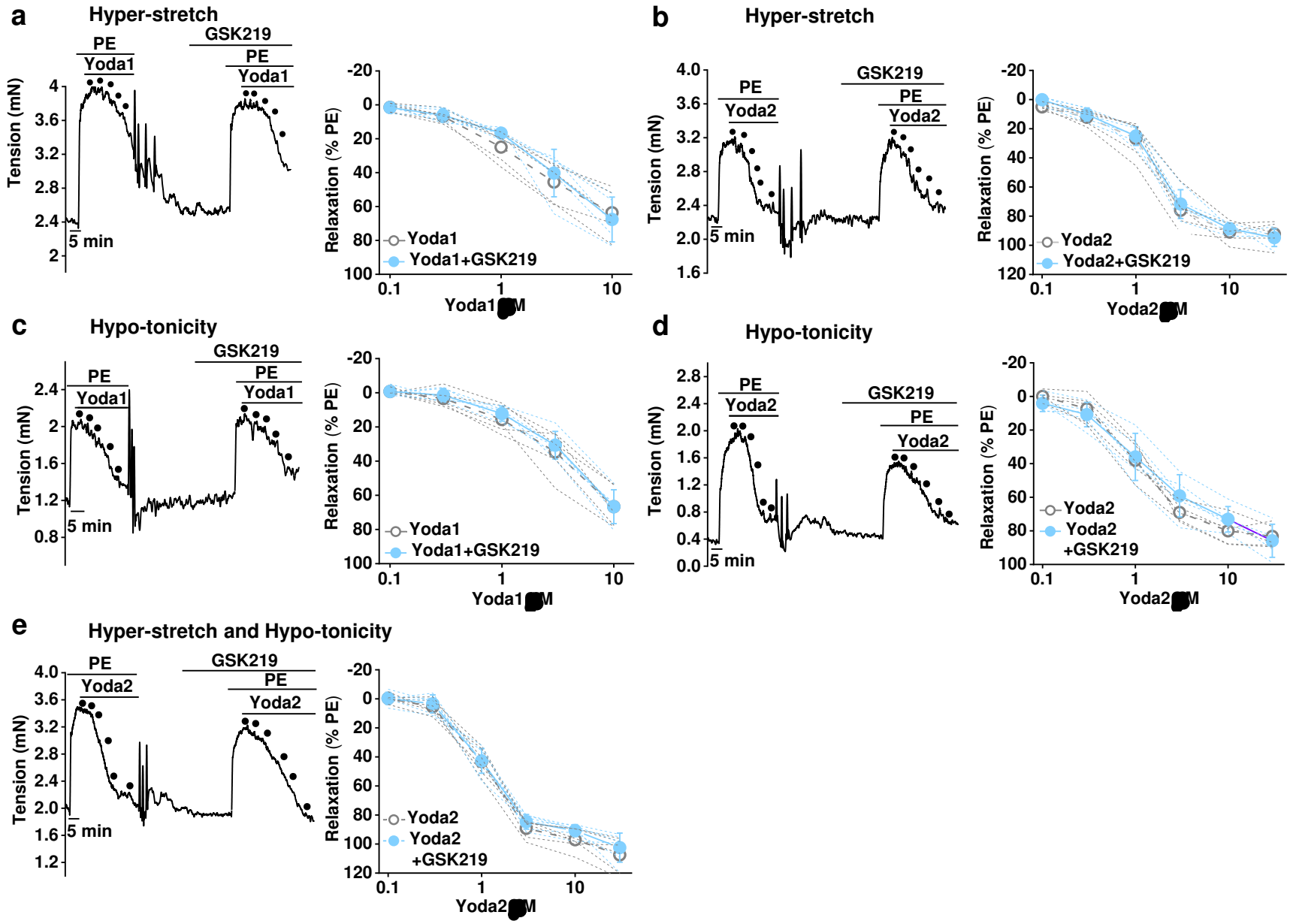
a
Hyper-stretch
PE
Yoda1
GSK219
PE
Yoda1
Tension (mN)
5 min
Relaxation (% PE)
Yoda1
Yoda1+GSK219
Yoda1 μM
b
Hyper-stretch
PE
Yoda2
GSK219
PE
Yoda2
Tension (mN)
5 min
Relaxation (% PE)
Yoda2
Yoda2+GSK219
Yoda2 μM
c
Hypo-tonicity
PE
Yoda1
GSK219
PE
Yoda1
Tension (mN)
5 min
Relaxation (% PE)
Yoda1
Yoda1+GSK219
Yoda1 μM
d
Hypo-tonicity
PE
Yoda2
GSK219
PE
Yoda2
Tension (mN)
5 min
Relaxation (% PE)
Yoda2
Yoda2
+GSK219
Yoda2 μM
e
Hyper-stretch and Hypo-tonicity
PE
Yoda2
GSK219
PE
Yoda2
Tension (mN)
5 min
Relaxation (% PE)
Yoda2
Yoda2
+GSK219
Yoda2 μM

SI Figure S7

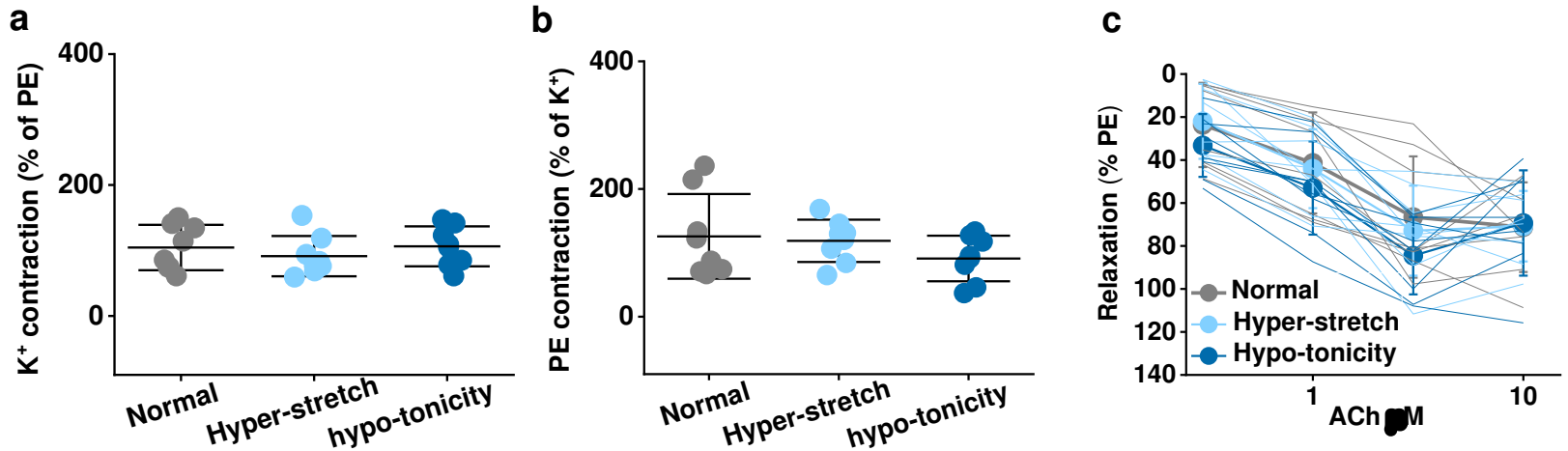
a
K+ contraction (% of PE)
400
200
0
Normal
Hyper-stretch
hypo-tonicity
b
PE contraction (% of K+)
400
200
0
Normal
Hyper-stretch
hypo-tonicity
c
Relaxation (% PE)
0
20
40
60
80
100
120
140
Normal
Hyper-stretch
Hypo-tonicity
1
10
ACh M